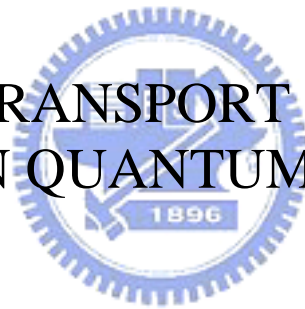# 國立交通大學

電子物理研究所

碩 士 論 文

開放式量子環中的量子傳輸

QUANTUM TRANSPORT THROUGH AN OPEN QUANTUM RING

研 究 生：陳淑娟

指導教授：朱仲夏

中華民國九十五年一月

開放式量子環中的量子傳輸

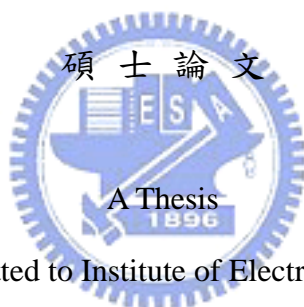# Quantum transport through an open quantum ring

研 究 生：陳淑娟　　　　　　　Student：Shu-Chuan Chen

指導教授：朱仲夏　　　　　　　Advisor：Dr. Chon-Saar Chu

國 立 交 通 大 學

電子物理研究所

碩 士 論 文

A Thesis

Submitted to Institute of Electrophysics

College of Science

National Chiao Tung University

in Partial Fulfillment of the Requirements

for the Degree of Master of Science

in

Electrophysics

January 2006

Hsinchu, Taiwan, Republic of China

中華民國九十五年一月

開放式量子環中的量子傳輸

研究生：陳淑娟　　　　　　　　　　　　　　指導教授：朱仲夏

國立交通大學電子物理研究所

摘要

本論文研究電子在開放式量子環中的傳輸特性。對於開放式量子環在零磁場時，我們可以發現其共振態符合封閉環的束縛態。並且當兩邊通道(lead)不對稱或是環的通道大小改變時，可以發現 Fano 結構。然而我們可以藉由改變環的對稱來調整 Fano 結構使其由寬變窄，亦可以讓環的通道變寬而使得 Fano 結構由窄變寬。在趨進一維的情形，共振峰變的較尖銳且向左移而接近封閉環的束縛態。對於開放式量子環在有限磁場下，我們可以發現 AB 效應(Aharonov-Bohm effect)而且其振盪周期為 $T_p = 2\Phi_0 = h/e$。然而值得注意的是在高磁場的情況下，並無周期振盪的情形。假如我們改變兩邊通道的相對角度，我們可以發現在高磁場的情況下改變角度變化較不大，但在低磁場的時候則是相反。

Quantum transport through an open quantum ring

Stusent: Shu-Chuan Chen   Advisors: Dr. Chon-Saar Chu

Institute of Electro-physics
National Chiao Tung University

Abstract

We study quantum transport properties of an open quantum ring(OQR). For the OQR in zero magnetic filed, we have found that the resonant peaks correspond to the bond states of a close ring. Fano structure in the transmission of an OQR can be found in two case which the two lead are configured asymmetrically and the channel size of ring is changed. Moreover, we can tune the Fano structure from broad to sharp by varying the symmetry of OQR and tune the Fano structure from sharp to broad by widening the channel width of the ring. Then approaching to 1D case, the resonance peaks become shaper and shift toward the left to be close to bound of close ring, when the channel narrow down. For the OQR with finite magnetic filed, We have found that the AB effect when the external field are applied in the ring and the oscillating period $T_p = 2\Phi_0 = h/e$. And it should be noted that the periodic oscillations are disappear at high magnetic field. If we change the angle θ of two lead for low and high magnetic field, we can found that it is sensitive to changing angle θ for small magnetic field but not for large magnetic field.

致謝

  在我的研究所生涯裡，要誠摯的感謝朱老師的指導，不管是做研究的態度亦或是在待人處事，老師都成為我很好的榜樣。此外，也特別謝謝唐志雄、鄒其君、王律堯學長與鐘淑維學長在研究上給我許多幫助與提醒。最後要感謝實驗室同學們，謝謝你們的陪伴與照顧。

Contents

List of Figures

Chapter 1

introduction

1.1 Introduction

In the past decade developments in mesoscopic physics have received much attention and made rapid progress. Quantum transport in the mesoscopic systems has been extensively studied both experimentally and theoretically. And the atomlike properties of dots or gate-confined quantum make them a good venue for studying the physics of confined carriers and many-body effects. Hence quantum dots have attracted considerable interest due to its potential to various application. They lead to interesting applications in fields such as quantum cryptography, quantum computing, optics, and optoelectronics, etc.

In recent work, however, a new geometry of semiconductor quantum rings has been introduced in experiments of magnetocapacitance and infrared excitation for few electrons [1, 2]. In many aspects, quantum rings are just quantum dots with a peculiar confining potential [3]. The decisive difference in their topology that the hole in their middle becomes prominent when an external magnetic field is applied. The magnetic flux that penetrates the interior of the ring will then determine the nature of the electronic states.

Since the pioneering publications in Ref.4, 5, the theoretical and experimental studies of ring interferometers are studied extensively. In ring geometries strongly connected to external leads the electron wave packets can take two different paths around the ring

which gives rise to interference. This can be associated with Young's double-slit experiment for photons. The electron in a ring geometry allows the relative phase of the electronic wave function in the two arms of the ring to be manipulated by a magnetic field perpendicular to the plane of the ring. And Aharonov and Bohm proposed such a setup to test experimentally the significance of the magnetic vector potential in quantum mechanics [6]. They predicted that the phase difference of the alternative paths changes by 2π as the flux through the ring is changed by one flux quantum h/q (q is the charge of the particle). Then magnetic field periodic resistance oscillations in ring structure have demonstrated that have a phase coherence length longer than or comparable to the perimeter by many experiments. Hence in mesoscopic physics the Aharonov-Bohm (AB) effect has become a standard tool to quantitatively investigate the phase coherence of transport in either metallic [7] or semiconducting systems [8–10]. Figure 1.1 shows the topography of a GaAs-AlGaAs heterostructure containing a two-dimensional electron gas below the surface.

In this thesis we study quantum transport properties of an open quantum ring(OQR). For simplicity, we ignore the effects of spins and the mutual interactions. Then we can found some interesting phenomena. If we change geometric configuration from symmetrical to asymmetrical of OQR, the Fano structures can be found in the transmission. Moreover the AB effect also can be observe in transmission of OQR with magnetic field. In the following , we would introduce the Fano effect and AB effect.

1.2 Fano effect

In 1961, Fano considered a physical situation which occurs in many systems addressed spectroscopically [11]. In the first part of the calculation, a quantum state, $|\phi\rangle$, with energy E_ϕ^0 , is taken to be coupled via matrix elements $V_{E'}$ to a continuum of states denoted by $|E'\rangle$, forming a resonance in the continuum. In the second part, a transition between another state, $|i\rangle$, (which is not resonant with the continuum) and the resonance is
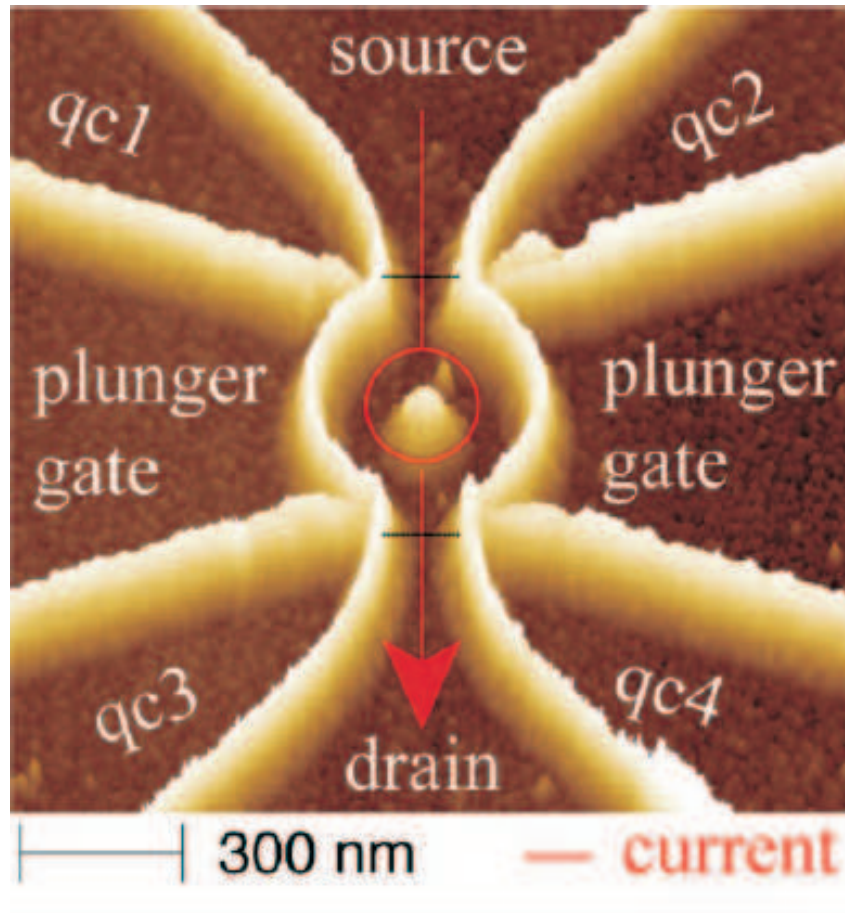
Figure 1.1: Micrograph of the quantum ring. The red line marks the current flow form source to drain through the two quantum point contacts angle the ring. The lateral gate electrodes termed qc1-qc4 are used to tune the tunnel barriers (indicate by dotted lines) connecting the quantum ring to its leads. The plunger gates allow the electron number on the ring to be controlled (adapted from Ref. 9)

considered, and it is shown that the interference between the contributions of the original continuum states and the resonance will always yields a characteristic asymmetric line shape in the transition probability. The typical phenomenon of Fano structures in which the transmission probabilities is downward dips to zero and soon rise up to one.

The Fano effect, a ubiquitous phenomenon observed in a large variety of experiments including neutron scattering [12], atomic photoionization [13], Raman scattering [14], and optical absorption [15]. While a statistically averaged nature of the system containing contributions from numerous sites is observed in these experiments, the Fano effect is essentially a single-impurity problem describing how a localized state embedded in the continuum acquires itinerancy over the system [16]. Therefore, an experiment on a single site would reveal this fundamental process in a more transparent way. While the single-site Fano effect has been reported in the scanning tunneling spectroscopy study of an atom on the surface [17, 18] or in transport through a quantum dot (QD) [19], there is little, if any, controllability in either case since the coupling between the discrete level and the continuum is naturally formed.

1.3 AB effect

According to quantum physics, when two coherent electron waves travelling along distinct paths recombine, they will interfere. The outcome reflects a phase difference arising from the different lengths of the paths taken by the electrons. If a magnetic field penetrates the region between the two paths, it will cause an additional phase shift, and so will change the resulting interference - a phenomenon known as the Aharanov-Bohm effect [6]

In this section, we would discuses the Aharonov-Bohm (AB) effect for a ring-shaped conductor. Experimentally [8, 9], the conductance of the ring have been observed to oscillate as a function of the magnetic through the ring, see Fig. 1.2and Fig. 1.3. The fundamental period of the oscillations is found to be the flux quantum, $\Phi_0 = h/e$.
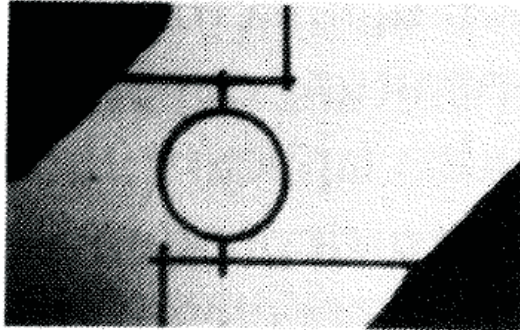
Figure 1.2: Transmission-electron micrograph of ring-shaped conductor [6]. The inside diameter of loop is 784 nm and the width of the wires is 41 nm (adapted from Ref.6).)
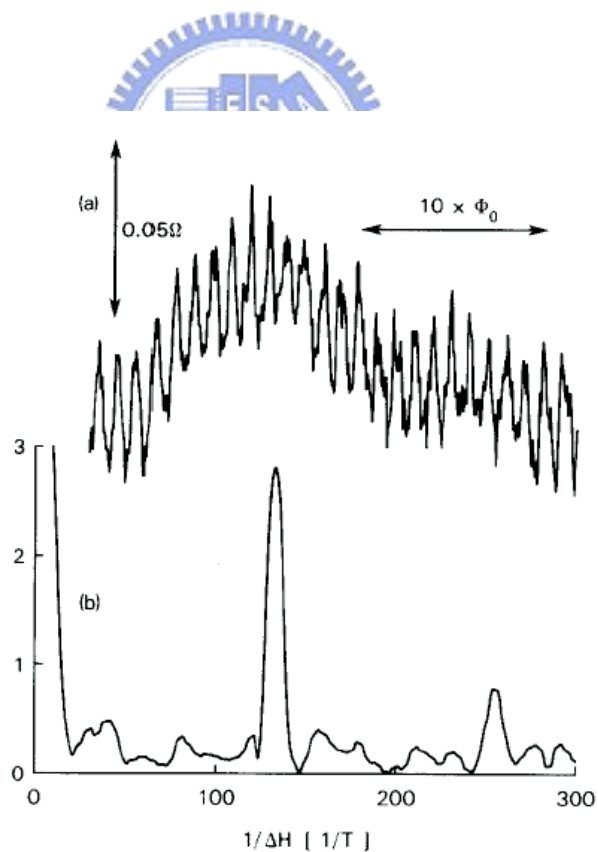
Figure 1.3: (a)Magnetoresistance of the above ring measured at $T = 0.01$K. (b)Fourier power spectrum in arbitrary units containing peaks at h/e and $h/2e$ (adapted from Ref.6).

5

The oscillations are caused by interference between the waves traversing the two branches of the ring (see Fig. 1.4).
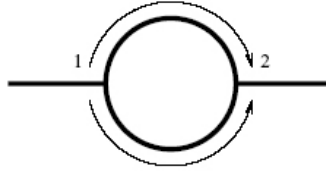
Figure 1.4: Aharonov-Bohm ring.

The phase shift in the upper branch of the ring is

$$\theta_{up} = \frac{|e|}{\hbar} \int_1^2 \overrightarrow{A} \cdot d\overrightarrow{r} \tag{1.1}$$

The fundamental period of the oscillations is found to be the flux quantum $\Phi_0 = \frac{\hbar}{|e|}$. By choosing in cylindrical coordinates $\overrightarrow{A} = \frac{1}{2}Br\overrightarrow{u_\phi}$ we obtain for the phase shift $\theta_{up} = \pi\frac{\Phi}{\Phi_0}$ where Φ is the total flux through the ring. Similarly, the phase shift in the lower branch is $\theta_{low} = -\pi\frac{\Phi}{\Phi_0}$.

The total phase difference between the waves in the different branches on the r.h.s. of the ring is thus $\theta = 2\pi\frac{\Phi}{\Phi_0}$. Consequently, the transmission probability oscillates with the period Φ_0. For example, if there is only one mode propagating in the ring, the transmission probability vanishes every time the phase shift equals an odd multiple of π.

In addition to the h/e-oscillations, there can also be observed subharmonic oscillations with frequencies h/ne, where n is an integer. These are caused by the waves traversing n times half of the ring in the same direction before interfering (now the total phase shift of the waves traversing, for example, in the clockwise direction is $\pi\frac{\Phi}{n\Phi_0}$).

Chapter 2

Theory and formulation

2.1 Landauer-Buttiker formalism

When the characteristic sizes of semiconductor devices are small in comparison with
the elastic mean free path of carriers, the carrier transport becomes ballistic [20]. The
Landauer-Buttiker formalism, which treats the transport as a scattering process, is par-
ticular useful for the description of transport thought a mesoscopic system in the ballistic
transport regime. And in this section, we introduce the multchannel Landauer-Buttiker
formalism starting from the single channel case [4].

Assume that there are two reservoir of electrochemical potential μ_1 and μ_2 respectively
connected by a 1D channel and there is a barrier in between the reservoirs. Consider two
reservoirs having the difference $\delta\mu = \mu_1 - \mu_2$ in the electrochemical potential. We assume
that electron coming into both side reservoirs form the 1D channel will not reflect back.
So, only those transmitted electrons in between $\delta\mu$ contribute to the current density J
from reservoir 1 to 2 in 1D, $J=I$.

In order to calculate the conductance we start from the equation of the current density
at zero temperature

$$I = -env_F \tag{2.1}$$

where v_F indicates Fermi velocity, n is the number of states per unit length that injected from reservior 1 to reservior 2, and considering the probability for transmission to be T, n can be written as

$$n = \left(\frac{dN}{dE}\right)(\mu_1 - \mu_2)T \tag{2.2}$$

For the density of state with 2 spin-states included, $(dN/dE) = 2/v_F$ in a 1D system (only one of the propagating direction is counted). Hence, we have

$$I = -\frac{2e}{h}\delta\mu T \tag{2.3}$$

Since the voltage difference $\delta V = \delta\mu/(-e)$, so that the conductance is in the form

$$G = \frac{2e^2}{h}T \tag{2.4}$$

For the case of multichannel system, we consider that electron propagate from the left nth subband transmitted into right mth subband, and assume the transmission probability as T_{nm}, and the reflection probability as R_{nm}. Therefore, the total transmission probability T_n and the total reflection probability R_n from the nth channel is

$$\begin{aligned} T_n &= \sum_m T_{nm} \\ R_n &= \sum_m R_{nm} \end{aligned} \tag{2.5}$$

By definition, the total current should be taken into account the contribution of all the incident subbands, $I_{tot} = \sum_n I_n$, where the I_n is related to the current transmission T_n, so we have

$$I_n = -\frac{2e}{h}\delta\mu \sum_m T_{nm} \tag{2.6}$$

and

$$I_{tot} = -\frac{2e}{h}\delta\mu\sum_n\sum_m T_{nm} \tag{2.7}$$

Following the Landaner-Buttiker formalism, the conductance can be expressed of the form

$$G = \frac{2e^2}{h}\sum_n\sum_m T_{nm} \tag{2.8}$$

2.2 Quantum transport through an open quantum ring with no magnetic field

In the section, we consider an open quantum ring with no external magnetic field, as is depicted in (Fig. 2.1).
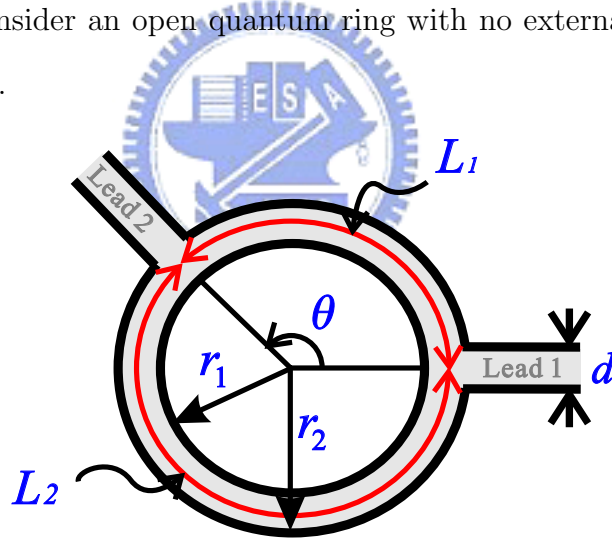
Figure 2.1: Schematic illustration of the ring

In the ring region, the Hamiltonian describing an electron inside the ring can be written of the form

$$H = \frac{\hbar^2}{2m*}\left[-\frac{\partial^2}{\partial r^2} - \frac{1}{r}\frac{\partial}{\partial r} - \frac{1}{r^2}\frac{\partial^2}{\partial\theta^2}\right] + V_r(r) \tag{2.9}$$

where m^* is the effective mass of electron, Vr (r) is the radial confinement potential. In

9

this case we adopt a hard-wall laterally confined model, namely,

$$
V_r(r) = \begin{cases} 0, r_1 \leq r \leq r_2 \\ \infty, r > r_2, r < r_1 \end{cases} \tag{2.10}
$$

And then we choose the energy unit $E^* = \hbar^2 k_F^2 / 2m*$, the length unit $a^* = 1/k_F$. Thus we can obtain the dimensionless Schrodinger Equation for ring:

$$
\left[-\frac{\partial^2}{\partial r^2} - \frac{1}{r}\frac{\partial}{\partial r} - \frac{1}{r^2}\frac{\partial^2}{\partial \theta^2} + V_r(r) \right] \psi_r(r, \theta) = E\psi_r(r, \theta) \tag{2.11}
$$

Here k_F is a typical Fermi wave vector in the reservoirs.

Taking the same units, we also can obtain the dimensionless Schrodinger Equation for leads as

$$
\left[-\frac{\partial^2}{\partial x^2} - \frac{\partial^2}{\partial y^2} + V_L(y) \right] \psi_L^{(i)}(x, y) = E\psi_L^{(i)}(x, y) \tag{2.12}
$$

$$
V_L(y) = \begin{cases} 0, 0 \leq y \leq d \\ \infty, y < 0, y > d \end{cases}
$$

where $i = 1$ for lead 1, $i = 2$ for lead 2, $V_L(y)$ is the confinement potential, and d is the width of lead.

By solve the Eq. (2.11) and Eq. (2.12), hence we can write down the wave function in each region:

$$
\begin{cases} \psi_L^{(1)}(x, y) = \sum_{n=1}^{N} (a_n^{(1)} e^{ik_n x} + b_n^{(1)} e^{-ik_n x})\sqrt{\frac{2}{d}} \sin\frac{n\pi y}{d}, \\ \psi_r(r, \theta) = \frac{1}{\sqrt{2\pi}} \sum_{m=-M}^{M} c_m \phi_m(kr)e^{im\theta} \\ \psi_L^{(2)}(x, y) = \sum_{n=1}^{N} (a_n^{(2)} e^{ik_n x} + b_n^{(2)} e^{-ik_n x})\sqrt{\frac{2}{d}} \sin\frac{n\pi y}{d} \end{cases} \tag{2.13}
$$

and

$$
\begin{cases}
\partial \psi_L^{(1)}/\partial x = \sum\limits_{n=1}^{N} (ik_n)(a_n^{(1)} e^{ik_n x} - b_n^{(1)} e^{-ik_n x}) \sqrt{\frac{2}{d}} \sin \frac{n\pi y}{d} \\
\partial \psi_r/\partial r = \frac{1}{\sqrt{2\pi}} \sum\limits_{m=-M}^{M} c_m \phi_m'(kr) e^{im\theta} \\
\partial \psi_L^{(2)}/\partial x = \sum\limits_{n=1}^{N} (ik_n)(a_n^{(2)} e^{ik_n x} - b_n^{(2)} e^{-ik_n x}) \sqrt{\frac{2}{d}} \sin \frac{n\pi y}{d}
\end{cases}
\tag{2.14}
$$

where n, m are both subband indices in the leads and the ring respectively. For the region of lead, d is the width of lead and the transverse energy levels are quantized, with $E_n = n^2 \pi^2/d^2$, so the wave vector for an electron with energy E and in the nth subband is given by $k_n = \sqrt{E - E_n}$. For the region of ring, $\phi_m(kr)$ is the radial wave function,

$$
\phi_m(kr) = J_m(kr) + \alpha_m Y_m(kr)
\tag{2.15}
$$

where $k = \sqrt{E}$, and $J_m(kr)$ and $Y_m(kr)$ are the Bessel functions of first and second kinds, respectively. Here $\phi_m(kr)$ satisfies the boundary condition $\phi_m(kr_1) = 0$, and hence

$$
\alpha_m = -J_m(kr_1)/Y_m(kr_1)
\tag{2.16}
$$

Now, by matching the wave function for the boundary conditions:

$$
\psi_L^{(1)}(0, y) + \psi_L^{(2)}(0, y) = \psi_r(r_2, \theta)
\tag{2.17}
$$

$$
\partial \psi_L^{(1)}/\partial x \Big|_{x=0} = \partial \psi_r/\partial r \big|_{r=r_2}
\tag{2.18}
$$

$$
\partial \psi_L^{(2)}/\partial x \Big|_{x=0} = \partial \psi_r/\partial r \big|_{r=r_2}
\tag{2.19}
$$

If we neglect the difference between the straight line of the channel and the arc line of the ring, and the angles to which the two side of two leads are θ_1, θ_2 and θ_3, θ_4 respectively,

hence we have

$$\sum_{n=1}^{N} (a_n^{(1)} + b_n^{(1)})\sqrt{\tfrac{2}{d}} \sin \tfrac{n\pi r_2(\theta-\theta_1)}{d} + \sum_{n=1}^{N} (a_n^{(2)} + b_n^{(2)})\sqrt{\tfrac{2}{d}} \sin \tfrac{n\pi r_2(\theta-\theta_3)}{d}$$
$$= \tfrac{1}{\sqrt{2\pi}} \sum_{m=-M}^{M} c_m \phi_m(kr)e^{im\theta} \qquad (2.20)$$

$$\sum_{n=1}^{N} (ik_n)(a_n^{(1)} - b_n^{(1)})\sqrt{\frac{2}{d}} \sin \frac{n\pi r_2(\theta-\theta_1)}{d} = \frac{1}{\sqrt{2\pi}} \sum_{m=-M}^{M} c_m \phi_m'(kr)e^{im\theta} \qquad (2.21)$$

$$\sum_{n=1}^{N} (ik_n)(a_n^{(2)} - b_n^{(2)})\sqrt{\frac{2}{d}} \sin \frac{n\pi r_2(\theta-\theta_3)}{d} = \frac{1}{\sqrt{2\pi}} \sum_{m=-M}^{M} c_m \phi_m'(kr)e^{im\theta} \qquad (2.22)$$

In the first stage, let us multiply both sides of Eq. (2.20) by the factor $(1/\sqrt{2\pi})e^{-im'\theta}$.
Here $m' = 0, \pm 1, \pm 2 \cdots \pm M$, and integrate from zero to 2π,

$$\sum_{n=1}^{N} (a_n^{(1)} + b_n^{(1)})I_{-m'n} + \sum_{n=1}^{N} (a_n^{(2)} + b_n^{(2)})\tilde{I}_{-m'n} = c_{m'}\phi_{m'}(kr_2), m' = 0, \pm 1, \pm 2, ..., \pm M$$
$$(2.23)$$

Then, we multiply both sides of Eq. (2.21) and Eq. (2.22) by $\sqrt{2/d}\sin n'\pi r_2(\theta-\theta_1)/d$
and $\sqrt{2/d}\sin n'\pi r_2(\theta-\theta_3)/d$, respectively. Here $n' = 1, 2 \cdots N$, and integrate from θ_1
to θ_2,

$$\sum_{n=1}^{N} (ik_n)(a_n^{(1)} - b_n^{(1)})U_{n'n} = \sum_{m=-M}^{M} c_m \phi_m'(kr_2)I_{mn'}, n' = 1, 2, ..., N \qquad (2.24)$$

$$\sum_{n=1}^{N} (ik_n)(a_n^{(2)} - b_n^{(2)})\tilde{U}_{n'n} = \sum_{m=-M}^{M} c_m \phi_m'(kr_2)\tilde{I}_{mn'}, n' = 1, 2, ..., N \qquad (2.25)$$

where

$$I_{\pm mn} = \sqrt{\frac{1}{\pi d}} \int_{\theta_1}^{\theta_2} \sin \frac{n\pi r_2(\theta-\theta_1)}{d} e^{\pm im\theta} d\theta \qquad (2.26)$$

$$\tilde{I}_{\pm mn} = \sqrt{\frac{1}{\pi d}} \int_{\theta_3}^{\theta_4} \sin \frac{n\pi r_2(\theta-\theta_3)}{d} e^{\pm im\theta} d\theta \qquad (2.27)$$

$$U_{n'n} = \frac{2}{d} \int_{\theta_1}^{\theta_2} \sin \frac{n'\pi r_2 (\theta - \theta_1)}{d} \sin \frac{n\pi r_2 (\theta - \theta_1)}{d} d\theta \tag{2.28}$$

$$\tilde{U}_{n'n} = \frac{2}{d} \int_{\theta_3}^{\theta_4} \sin \frac{n'\pi r_2 (\theta - \theta_3)}{d} \sin \frac{n\pi r_2 (\theta - \theta_3)}{d} d\theta \tag{2.29}$$

In Eq. (2.13) $b_n^{(1)}$ and $b_n^{(2)}$ are coefficients of electron waves traveling inward or increasing exponentially with x (for imaginary k_n), which are all set to be zero according to physical consideration, except one coefficient $b_i^{(1)} = 1/\sqrt{k_i}$, representing the amplitude of one injected wave. And the coefficients $a_n^{(1)}$ and $a_n^{(2)}$ which are related to the transmission and reflection amplitudes. Hence we have 2M+2N+1 equations Eq. (2.23)-Eq. (2.25) for 2M+2N+1 unknown coefficients $a_n^{(1)}$, $a_n^{(2)}(n' = 1, 2, ...N)$ and $c_m(m = 0, \pm1, ... \pm M)$.

Rewrite the Eq. (2.23)-Eq. (2.25) in matrix form

$$\mathrm{I}_0(A + B) + \tilde{\mathrm{I}}_0(A' + B') = \Phi C \tag{2.30}$$

$$i\mathrm{UK}(A - B) = \mathrm{I}_1\Phi'C \tag{2.31}$$

$$i\tilde{\mathrm{U}}\mathrm{K}(A' - B') = \tilde{\mathrm{I}}_1\Phi'C \tag{2.32}$$

where

Solving the set of equations we obtain the coefficients $a_n^{(1)}$ and $a_n^{(2)}$:

$$a_n^{(1)} = \frac{r_{ni}}{\sqrt{k_n}} \tag{2.33}$$

$$a_n^{(2)} = \frac{t_{ni}}{\sqrt{k_n}} \tag{2.34}$$

The total transmission and reflection probabilities are given by

$$T = \sum_{ni} |t_{ni}|^2$$
$$R = \sum_{ni} |r_{ni}|^2 \tag{2.35}$$

which conservation condition holds for $T + R = 1$

Moreover, the conductance G can be found by the expression

$$G = \frac{2e^2}{h}T \tag{2.36}$$

2.3 Quantum transport through an open quantum ring in a magnetic field

In the section, we consider an open quantum ring applied by an external perpendicular magnetic field, while the two leads without magnetic field.

In the region of ring, the Hamiltonian of an electron in a ring with a magnetic field B is given by

$$
\begin{aligned}
H &= \frac{1}{2m*} \left(P + eA \right)^2 + V_r(r) \\
&= \frac{1}{2m*} \left(P^2 + e \left(P \cdot A + A \cdot P \right) + e^2 A^2 \right) + V_r(r)
\end{aligned}
\tag{2.37}
$$

where m^* is the effective mass of electron, $V_r(r)$ is the radial confining potential. In this case, again, we consider the ring with hard-wall confinement described by

$$
V_r(r) = \begin{cases} 0, r_1 \leq r \leq r_2 \\ \infty, r > r_2, r < r_1 \end{cases}
\tag{2.38}
$$

and $\mathbf{A}$ is the magnetic vector potential such that $B = \nabla \times A$.

Assuming that the magnetic field is constant and perpendicular to the plane of the ring, the vector potential can be expressed in polar coordinates:

$$
A = \frac{B}{2} \left(0, r, 0 \right)
\tag{2.39}
$$

where $B = |B|$. Since the system is circularly symmetric it is convenient to write the

Hamiltonian in polar coordinates

$$H = \frac{\hbar^2}{2m*} \left[-\left(\frac{\partial^2}{\partial r^2} + \frac{1}{r}\frac{\partial}{\partial r} + \frac{1}{r^2}\frac{\partial^2}{\partial \theta^2} \right) - i\frac{eB}{\hbar}\left(\frac{\partial}{\partial \theta} \right) + \frac{1}{\hbar^2}\left(\frac{eB}{2} \right)^2 r^2 \right] + V_r(r) \quad (2.40)$$

Let $w_c = \frac{eB}{m^*}$, w_c being the cyclotron frequency, and then the Hamiltonian can be rewrite of the form

$$H = \frac{\hbar^2}{2m^*} \left[-\left(\frac{\partial^2}{\partial r^2} + \frac{1}{r}\frac{\partial}{\partial r} + \frac{1}{r^2}\frac{\partial^2}{\partial \theta^2} \right) - i\frac{1}{\hbar}m^* w_c \left(\frac{\partial}{\partial \theta} \right) + \frac{1}{\hbar^2}\frac{1}{4}(m^*)^2 w_c^2 r^2 \right] + V_r(r) \quad (2.41)$$

And then we choose the energy unit $E^* = \hbar^2 k_F^2/2m*$, the length unit $a^* = 1/k_F$, and $w_c^* = E^*/\hbar = \hbar k_F^2/2m*$. Therefore we can obtain the dimensionless Schrodinger equation describing the electronic transport through the open quantum ring, given by

$$\left[-\left(\frac{\partial^2}{\partial r^2} + \frac{1}{r}\frac{\partial}{\partial r} + \frac{1}{r^2}\frac{\partial^2}{\partial \theta^2} \right) - i\frac{1}{2}w_c\left(\frac{\partial}{\partial \theta} \right) + \frac{1}{16}(w_c)^2 r^2 + V_r(r) \right] \psi_r(r,\theta) = E\psi_r(r,\theta)$$
$$(2.42)$$

Assuming the eigenfunction can be written as

$$\psi_r(r,\theta) = \frac{e^{im\theta}}{\sqrt{2\pi}} R_m(r) \quad (2.43)$$

Substituting Eq. (2.43) into Eq. (2.42), we have

$$\left[-\left(\frac{\partial^2}{\partial r^2} + \frac{1}{r}\frac{\partial}{\partial r} \right) + \left(\frac{m^2}{r^2} \right) + \frac{1}{2}mw_c + \frac{1}{16}(w_c)^2 r^2 \right] R_m(r) = ER_m(r) \quad (2.44)$$

$$\Rightarrow \left[\left(\frac{\partial^2}{\partial r^2} + \frac{1}{r}\frac{\partial}{\partial r} \right) - \left(\frac{m^2}{r^2} \right) + \left(E - \frac{1}{2}mw_c \right) - \frac{1}{16}(w_c)^2 r^2 \right] R_m(r) = 0 \quad (2.45)$$

Then we assume

$$R_m(r) \sim r^{|m|} e^{-(w_c r^2)/8} u(r) = r^{|m|} e^{-ar^2} u(r) \quad (2.46)$$

15

here $a = w_c/8$.

Substituting Eq. (2.46) into Eq. (2.45), we can obtain

$$\left\{ \frac{\partial^2 u(r)}{\partial r^2} + \left((2\,|m| + 1)\, r^{-1} + \left(-\frac{w_c}{2} \right) r \right) \frac{\partial u(r)}{\partial r} + \left[(2\,|m| + 2) \left(-\frac{w_c}{4} \right) + \left(E - \frac{1}{2} m w_c \right) \right] \right\} u(r) = 0 \tag{2.47}$$

Now, let $x = 2ar^2 = \frac{w_c}{4} r^2$, so we get

$$\frac{\partial x}{\partial r} = w_c r/2 \tag{2.48}$$

$$\frac{\partial^2 x}{\partial^2 r} = w_c/2 \tag{2.49}$$

$$\frac{\partial u(r)}{\partial r} = \frac{\partial x}{\partial r} \frac{du(x)}{dx} = \frac{w_c}{2} r \frac{du(x)}{dx} \tag{2.50}$$

$$\frac{\partial^2 u(r)}{\partial r^2} = \frac{\partial^2 x}{\partial^2 r} \frac{du(x)}{dx} + \left(\frac{\partial x}{\partial r} \right)^2 \frac{d^2 u(x)}{dx^2} = \frac{w_c}{2} \frac{du(x)}{dx} + \left(\frac{w_c}{2} \right)^2 r^2 \frac{d^2 u(x)}{dx^2} \tag{2.51}$$

Substituting Eq. (2.48)-Eq. (2.51) into Eq. (2.47), we have

$$\left\{ x \frac{d^2 u(x)}{dx^2} + \{ ((|m| + 1) - x) \} \frac{du(x)}{dx} + \underbrace{\left[\left(\frac{E}{w_c} - \frac{1}{2} \frac{m w_c}{w_c} \right) - \frac{1}{2} (|m| + 1) \right]}_{\varepsilon_m} \right\} u(x) = 0 \tag{2.52}$$

where

$$\varepsilon_m = \left(\frac{E}{w_c} - \frac{1}{2} m \right) - \frac{1}{2} (|m| + 1) \tag{2.53}$$

Eq. (2.52) is the form of confluent hypergeometric equation, namely that the $u(x)$ is the so-called confluent hypergeometric function, give by

$$u(x) = c_m M \left(-\varepsilon_m, |m| + 1; \frac{w_c}{4} r^2 \right) + d_m U \left(-\varepsilon_m, |m| + 1; \frac{w_c}{4} r^2 \right) \tag{2.54}$$

It is now easy to obtain the $R(r)$ by substituting Eq. (2.54) into Eq. (2.46):

$$
\begin{aligned}
R_m(r) &= r^{|m|}\left(c_m M(-\varepsilon_m, |m|+1; \tfrac{w_c}{4}r^2) + d_m U(-\varepsilon_m, |m|+1; \tfrac{w_c}{4}r^2)\right) e^{-w_c r^2/8} \\
&= c_m r^{|m|}\left(M(-\varepsilon_m, |m|+1; \tfrac{w_c}{4}r^2) + \alpha_m U(-\varepsilon_m, |m|+1; \tfrac{w_c}{4}r^2)\right) e^{-w_c r^2/8} \\
&= c_m \phi_m(r)
\end{aligned}
\tag{2.55}
$$

where M , U are the confluent hypergeometric functions of first and second kinds, respectively. The $R_m(r)$ satisfies the boundary condition $R_m(r_1) = 0$, and hence

$$
\alpha_m = -M(-\varepsilon_m, |m|+1; \frac{w_c}{4}r_1^2)/U(-\varepsilon_m, |m|+1; \frac{w_c}{4}r_1^2)
\tag{2.56}
$$

Hence the wavefunction which in the region of ring is written as

$$
\psi_r(r,\theta) = \frac{1}{\sqrt{2\pi}} \sum_m c_m \phi_m(r) e^{im\theta}
\tag{2.57}
$$

Utilizing this equation, itis easy to caculate the total transmission and reflection probabilities of the open ring system by matching boundary condition which is the same as the method in Sec. 2.2.

2.4 Quantum transport through an open quantum ring with a magnetic flux

In the section, we consider an open quantum ring with a magnetic flux in center of ring.

Assuming that the magnetic flux is constant and in the center region of ring, the vector potential can be expressed :

$$
\begin{cases}
A_\varphi = \Phi/2\pi r \\
A_r = 0 \\
A_z = 0
\end{cases}
\tag{2.58}
$$

Hamiltonian:

$$
\begin{aligned}
H &= \tfrac{1}{2m*} \left(\mathrm{P} + e\mathrm{A} \right)^2 + V_r(r) \\
&= \tfrac{1}{2m*} \left(\mathrm{P}^2 + e \left(\mathrm{P} \cdot \mathrm{A} + \mathrm{A} \cdot \mathrm{P} \right) + e^2 \mathrm{A}^2 \right) + V_r(r)
\end{aligned}
\tag{2.59}
$$

where $m*$ is the effective mass of electron, $V_r(r)$ is the radial confining potential. In this case, again, we consider the ring with hard-wall confinement described by

$$
V_r(r) = \begin{cases} 0, r_1 \le r \le r_2 \\ \infty, r > r_2, r < r_1 \end{cases}
\tag{2.60}
$$

Since the system is circularly symmetric it is convenient to write the Hamiltonian in polar coordinates:

$$
H = \frac{\hbar^2}{2m*} \left[-\left(\frac{\partial^2}{\partial r^2} + \frac{1}{r}\frac{\partial}{\partial r} + \frac{1}{r^2}\frac{\partial^2}{\partial \theta^2} \right) - i2\frac{e}{\hbar}\left(\frac{\Phi}{2\pi r}\frac{1}{r}\frac{\partial}{\partial \theta} \right) + \left(\frac{e}{\hbar}\frac{\Phi}{2\pi r} \right)^2 \right] + V_r(r)
\tag{2.61}
$$

Let $\alpha = \frac{e}{\hbar}\frac{\Phi}{2\pi} = \frac{\Phi}{2\Phi_0}$, Φ being the magnetic flux, and defining $\Phi_0 = \frac{h}{2e}$ as the flux quantum, then the Hamiltonian can be rewrite of the form

$$
H = -\frac{\hbar^2}{2m*} \left[\frac{\partial^2}{\partial r^2} + \frac{1}{r}\frac{\partial}{\partial r} + \frac{1}{r^2}\left(\frac{\partial^2}{\partial \theta^2} + i2\alpha\frac{\partial}{\partial \theta} - \alpha^2 \right) \right] + V_r(r)
\tag{2.62}
$$

And then we choose the energy unit $E^* = \hbar^2 k_F^2 / 2m*$, and the length unit $a^* = 1/k_F$. Therefore we can obtain the dimensionless Schrodinger equation describing the electronic transport through the open quantum ring, given by

$$
\left[-\left(\frac{\partial^2}{\partial r^2} + \frac{1}{r}\frac{\partial}{\partial r} + \frac{1}{r^2}\left(\frac{\partial^2}{\partial \theta^2} + i2\alpha\frac{\partial}{\partial \theta} - \alpha^2 \right) \right) + V_r(r) \right] \psi_r(r,\theta) = E\psi_r(r,\theta)
\tag{2.63}
$$

Eq. (2.63) can be rewritten as

$$
\left(r^2\frac{\partial^2}{\partial r^2} + r\frac{\partial}{\partial r} + r^2\left(E - V_r(r) \right) \right) \psi_r(r,\theta) = -\left(\frac{\partial^2}{\partial \theta^2} + i2\alpha\frac{\partial}{\partial \theta} - \alpha^2 \right) \psi_r(r,\theta)
\tag{2.64}
$$

Assuming the eigenfunction can be written as

$$\psi_r(r,\theta) = R(r)\Theta(\theta) \tag{2.65}$$

Substituting Eq. (2.65) into Eq. (2.64), we have

$$\frac{1}{R(r)}\left(r^2\frac{\partial^2}{\partial r^2} + r\frac{\partial}{\partial r} + r^2\left(E\right)\right)R(r) = -\frac{1}{\Theta(\theta)}\left(\frac{\partial^2}{\partial\theta^2} + i2\alpha\frac{\partial}{\partial\theta} - \alpha^2\right)\Theta(\theta) \tag{2.66}$$

First, we let

$$-\frac{1}{\Theta(\theta)}\left(\frac{\partial^2}{\partial\theta^2} + i2\alpha\frac{\partial}{\partial\theta} - \alpha^2\right)\Theta(\theta) = d^2 \tag{2.67}$$

and assume

$$\Theta(\theta) = \frac{1}{\sqrt{2\pi}}e^{i(m'-\alpha)\theta} \tag{2.68}$$

Substituting Eq. (2.68) into RHS of Eq. (2.67):

$$
\begin{aligned}
&-\frac{1}{e^{i(m'-\alpha)\theta}}\left(\frac{\partial^2}{\partial\theta^2} + i2\alpha\frac{\partial}{\partial\theta} - \alpha^2\right)e^{i(m'-\alpha)\theta}\\
&= -\frac{1}{e^{i(m'-\alpha)\theta}}\left(\left(i\left(m'-\alpha\right)\right)^2 e^{i(m'-\alpha)\theta} + i2\alpha\left(i\left(m'-\alpha\right)\right)e^{i(m'-\alpha)\theta} - \alpha^2 e^{i(m'-\alpha)\theta}\right)\\
&= -\left(\left(i\left(m'-\alpha\right)\right)^2 + i2\alpha\left(i\left(m'-\alpha\right)\right) - \alpha^2\right)\\
&= -\left(-\left(m'^2 - 2m'\alpha + \alpha^2\right) - 2m'\alpha + 2\alpha^2 - \alpha^2\right)\\
&= -\left(-m'^2\right) = m'^2
\end{aligned}
\tag{2.69}
$$

hence, $d^2 = m'^2$.

The boundary condition of $\Theta(\theta)$ is

$$\Theta(\theta) = \Theta(\theta + 2\pi) \tag{2.70}$$

Substituting Eq. (2.68) into Eq. (2.70), we can obtain

$$e^{i(m'-\alpha)2\pi} = 0 \tag{2.71}$$

Hence, $m' - \alpha = 0, \pm 1, \pm 2 \cdots \pm M$.

Then Eq. (2.66) can be rewritten as

$$\frac{1}{R(r)} \left(r^2 \frac{\partial^2}{\partial r^2} + r \frac{\partial}{\partial r} + r^2 (E) \right) R(r) = m'^2 \tag{2.72}$$

For any m'

$$\left(r^2 \frac{\partial^2}{\partial r^2} + r \frac{\partial}{\partial r} + r^2 E - m'^2 \right) R_{m'}(r) = 0 \tag{2.73}$$

Now, let $k = \sqrt{E}$ and $t = kr$, so Eq. (2.73) become

$$\frac{\partial^2 R_{m'}(t)}{\partial t^2} + \frac{1}{t} \frac{\partial R_{m'}(t)}{\partial t} + (1 - \frac{m'^2}{t^2}) R_{m'}(t) = 0 \tag{2.74}$$

Eq. (2.74) is the form of bessel equation, hence $R_{m'}(kr)$ give by

$$R_{m'}(kr) = \begin{cases} c_{m'} \left(J_{m'}(kr) + \alpha_{m'} N_{m'}(kr) \right), m' = 0, \pm 1, \pm 2 \cdots \pm M \\ c_{m'} \left(J_{m'}(kr) + \alpha_{m'} J_{-m'}(kr) \right), \text{other} \end{cases} \tag{2.75}$$

where $J_{m'}(kr)$ and $Y_{m'}(kr)$ are the Bessel functions of first and second kinds, respectively. Here $R_{m'}(kr)$ satisfies the boundary condition $R_{m'}(kr_1) = 0$, and hence

$$\alpha_{m'} = \begin{cases} -J_{m'}(kr_1)/N_{m'}(kr_1), m' = 0, \pm 1, \pm 2 \cdots \pm M \\ -J_{m'}(kr_1)/J_{-m'}(kr_1), \text{other} \end{cases} \tag{2.76}$$

Let $m' - \alpha = m = 0, \pm 1, \pm 2, L, \pm M$, so Eq. (2.75) become

$$R_{m'}(kr) = \begin{cases} c_m \left(J_{m+\alpha}(kr) + \alpha_m N_{m+\alpha}(kr) \right), m + \alpha = 0, \pm 1, \pm 2 \cdots \pm M \\ c_m \left(J_{m+\alpha}(kr) + \alpha_m J_{-(m+\alpha)}(kr) \right), \text{other} \end{cases} = c_m \phi_{m+\alpha}(kr)$$

(2.77)

Hence the wavefunction which in the region of ring is written as

$$\psi_r(r) = R(r)\Theta(\theta) = \frac{1}{\sqrt{2\pi}} \sum_{m=-M}^{M} c_m \phi_{m+\alpha}(kr) e^{im\theta}$$

(2.78)

Utilizing this equation, it is easy to calculate the total transmission and reflection probabilities of the open ring system by matching boundary condition which is the same as the method in Sec. 2.1.

Chapter 3

Result and discussion of open quantum ring without magnetic field

We already derive the transmission probabilities of an open quantum ring (OQR) matching method. And the electronic transmission and the electron wave function can be exactly calculated numerically. In this chapter, we would like to show our results of electronic transport through an OQR of $r_2 = 2$, $r_1 = 1$, $s = 1$. And then we vary the angle (θ) of the two lead and the channel size of ring, the result are shown in the section 3.2. Finally, we approach our result to 1-D case.

3.1 Mesoscopic transport properties of an open quantum ring

The coefficient of electron transmission through the open quantumnh ring in zero magnetic field was calculated in Chap.2. As shown in Fig. 3.1, the transmission probabilities T (solid line) as a functions of the momentum of injected electron for an OQR of $r_2 = 2$, $r_1 = 1$, $s = 1$ and $\theta = \pi$. Here, we just consider the momentum of the range from 1 to 2, only first subband contributes to the transmission. The solid line refers transmission probabilities and the dashed line refers the momentum of confined states in the closed

ring. Here, n and m are the radial and angular quantum number, respectively.

In Fig. 3.1, for the solid line, there are seven peaks and dips, the maximum value is one for each peak and the minimum value of dip is form of envelope. And the momentum of those peaks are 1.032, 1.127, 1.266, 1.434, 1.618, 1.80 and 1.96, the momentum of those dip are 1.063, 1.185, 1.344, 1.529, 1.723, 1.929 and 1.977. And for the dashed line, there are eight confined states of close ring, we denote them as $(n,m) = (1,1)(1,2)...(1,8)$, respectively.

From the Fig. 3.1, we observe that the peaks are sharper and they also match better with confined states when the momentum k are near the subband of lead ($k=1,2$). And we can found that there are eight dashed line, but there are only seven peaks, it seems that one peak in the transmission is missing. In order to understand the incident electron behavior in space, hence we plot wave function probability at the maximum value of peak. They are shown in Fig. 3.2. Comparing Fig. 3.2(a)-(g), we can found that the wave function at $k=$ 1.032(a), 1.127(b), 1.266(c) and 1.344(d), the number of waves in the ring are 1, 2, 3 and 4, respectively. And directly perceived through the senses, it seems that the number of waves in the ring at $k=1.618$(e) shall be 5 by sense, but from the Fig. 3.2(e), we can see that there are 6 waves in the ring at $k=1.618$. So we can know that the peak of missing shall between $k=1.4339$ and 1.618. And the scale of wavefunctioin probability in the ring for $k=1.032$ and 1.8 are larger than lead. However, it seems that the electron like to stay in the ring relatively.

3.2 Tuning of the Fano resonance in an open quantum ring

3.2.1 Effect of symmetrically to asymmetrically

Fano structure in the transmission of an OQR can be found in two case which the two lead are configured asymmetrically and the channel size of ring is changed. First, we consider
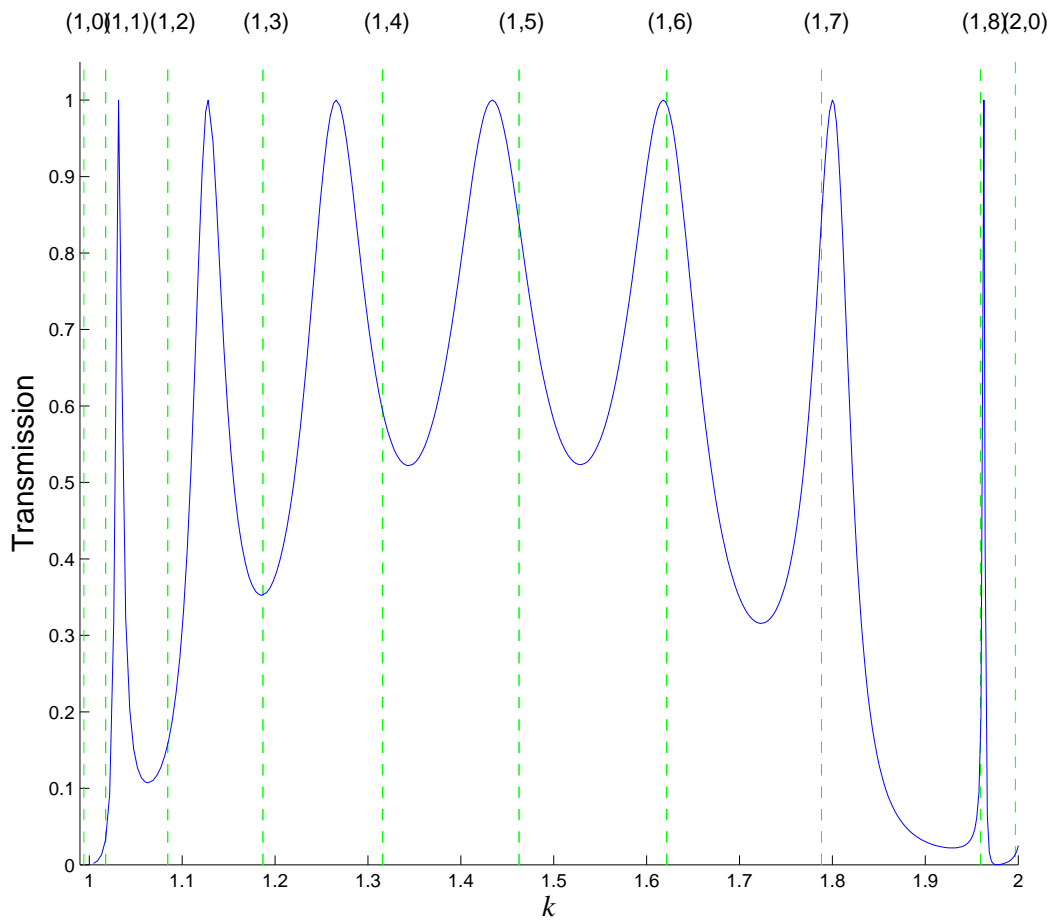
Figure 3.1: The solid line refers transmission probabilities as functions of the electron momentum for an OQR of $r_2 = 2$, $r_1 = 1$, $s = 1$ and $\theta = \pi$. The dashed line refers the momentum of confined states in the closed ring. The n and m is the radial and angular quantum number, respectively.
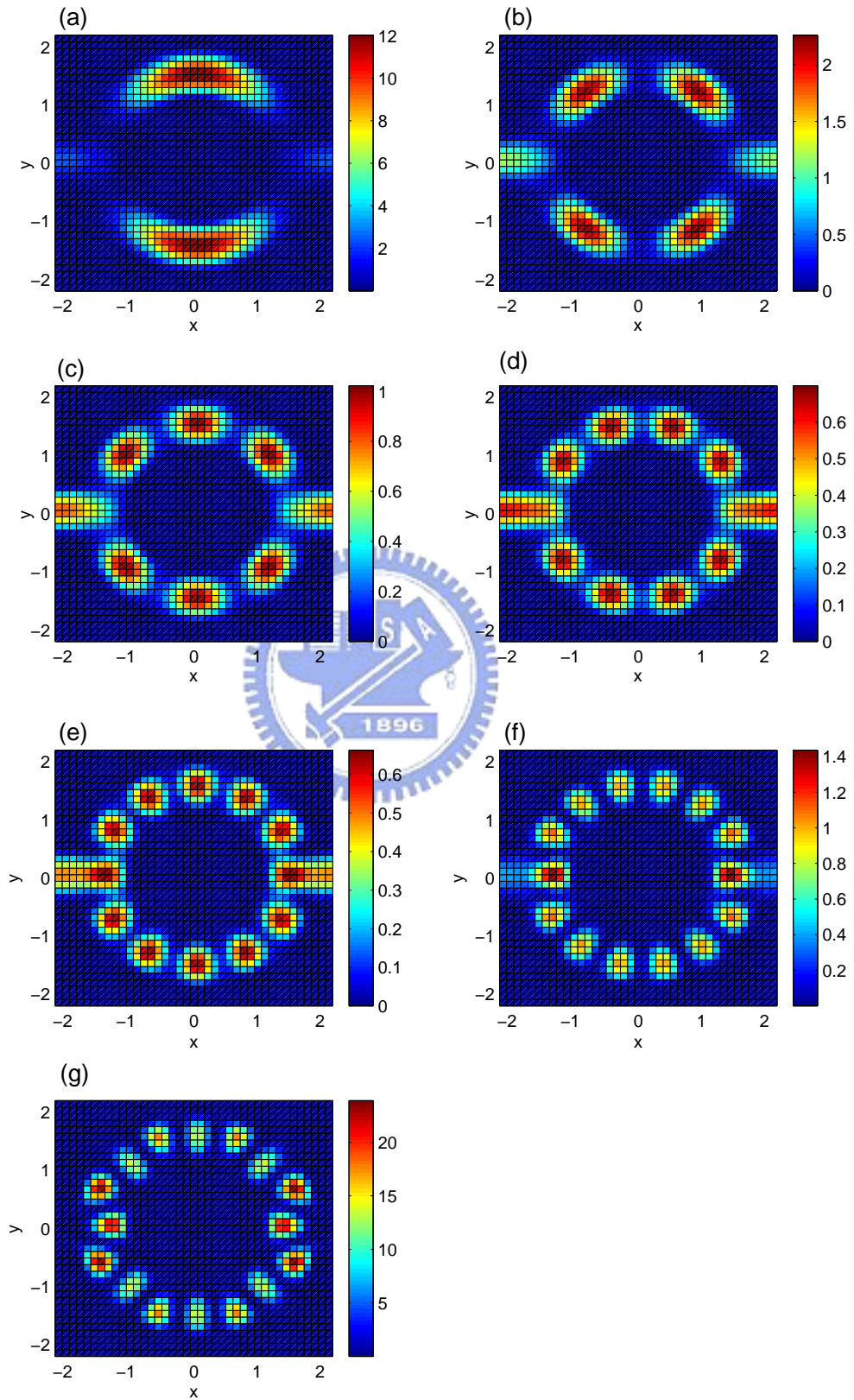
Figure 3.2: The wave function of k=1.032(a), 1.127(b), 1.266(c), 1.434(d), 1.618(e), 1.8(f), 1.96(g) for $r_2 = 2$, $r_1 = 1$, $s = 1$ and $\theta = \pi$

the case that two lead are configured asymmetrically, that is shown in Fig. 3.3 From
Fig. 3.3, we see that the typical phenomenon of Fano structures in which the transmission
probabilities manifests downward dips to zero and soon rise up to one, when we vary the
angle (θ) of two lead. And those Fano structures are near confined states of the closed
ring. When θ are varied continuously, the Fano peak seems to become broader. Hence, we
can tune the Fano resonance by varying the geometric parameters such that the quantum
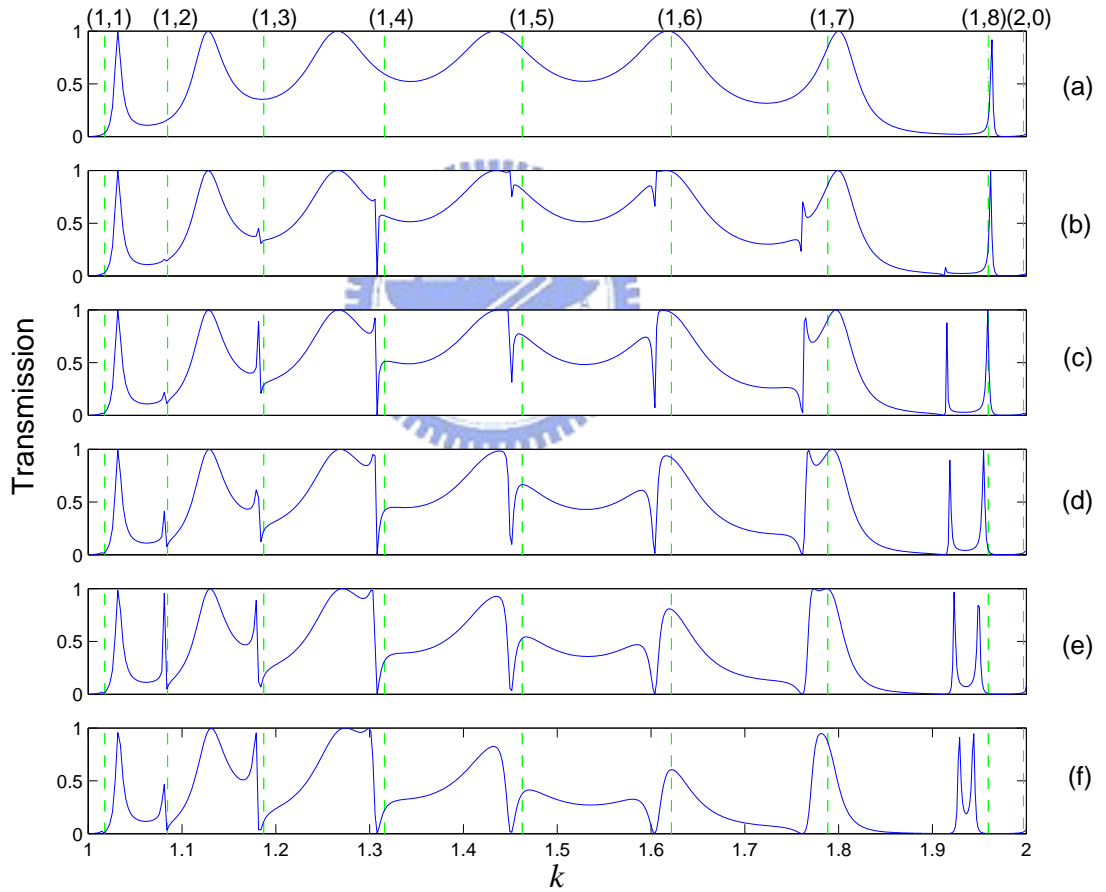ring is either symmetric to asymmetric.

Figure 3.3: Current transmission as a function of the electron momentum of the OQR of
$r_2 = 2$, $r_1 = 1$, $s = 1$, for different angle $\theta = \pi$(a), 0.99π(b), 0.98π(c), 0.97π(d), 0.96π(e),
0.95π(f).

3.2.2 Effects of varying channel size of ring

According to section 3.2.1, we can tune the Fano peak by varying the angle of two lead. But in the experiment, it's hard to varying the angle of lead. So we try to vary other parameter to see if there are still Fano peaks. Consequently, we find that Fano peak occur as varying the channel size of ring. Then, we vary the channel size of ring by changing r_1 from 1 to 0.95 and fix the $r_2 = 2$ and $s = 1$. The transmission probability for each r_1 is shown in Fig.3.2.2. Comparing Fig. 3.4(a)-(f), we can see that the Fano structures appear at the momentum after k=1.9 in Fig. 3.4(d). Before k=1.9 in Fig. 3.4(a)-(f), the profile just shift forward to low momentum. And the shift of profile just like the shift of the confined momentum of close ring (dashed line) before k=1.9 in Fig. 3.4(a)-(f). It is interesting to see if there is any significant difference before k=1.9 and after k=1.9 in Fig. 3.4. Consequently, we observe in Fig. 3.4 that the Fano structures appear near the confined state (1,8) of close ring in Fig. 3.4(d)-(f). And the different of Fig. 3.4(a)-(c) and (d)-(f) is that the confined state (1,8) is beyond the (2,0) in Fig. 3.4(d)-(f) but not in Fig. 3.4(a)-(e). And the Fano peak become shaper, when we vary the channel size from 1 to 0.95.

3.3 Approach to 1D rings

Here, we approach our result to 1D case and we just consider energy below the second subband and that particle propagates only within the first subband. In order to comparing more convenient, we use the longitudinal wave number $k_{//} = \sqrt{E - E_{CR}^0}$ instead of the momentum k, where E is total energy and E_{CR}^0 is the energy at confined state (1,0) of close ring. And we define $\lambda_{//} = 2\pi/k_{//}$ as the wavelength, and $L_{1,2} = R\theta_{1,2}$ as armlengths, here $R = (r_2 + r_1)/2$ and $\theta_{1,2}$ are the angles shown in Fig. 2.1. We compare the two cases of broad channel ($R/s = 3.5$) and narrow channel ($R/s = 9.5$), where s is the width of ring. The transmission venues $(L_1 + L_2)/\lambda_{//}$ at symmetrical arms ($L_1 = L_2$) in the ring is shown as Fig. 3.5. Form Fig. 3.5, it are seen that resonance peaks become shaper and
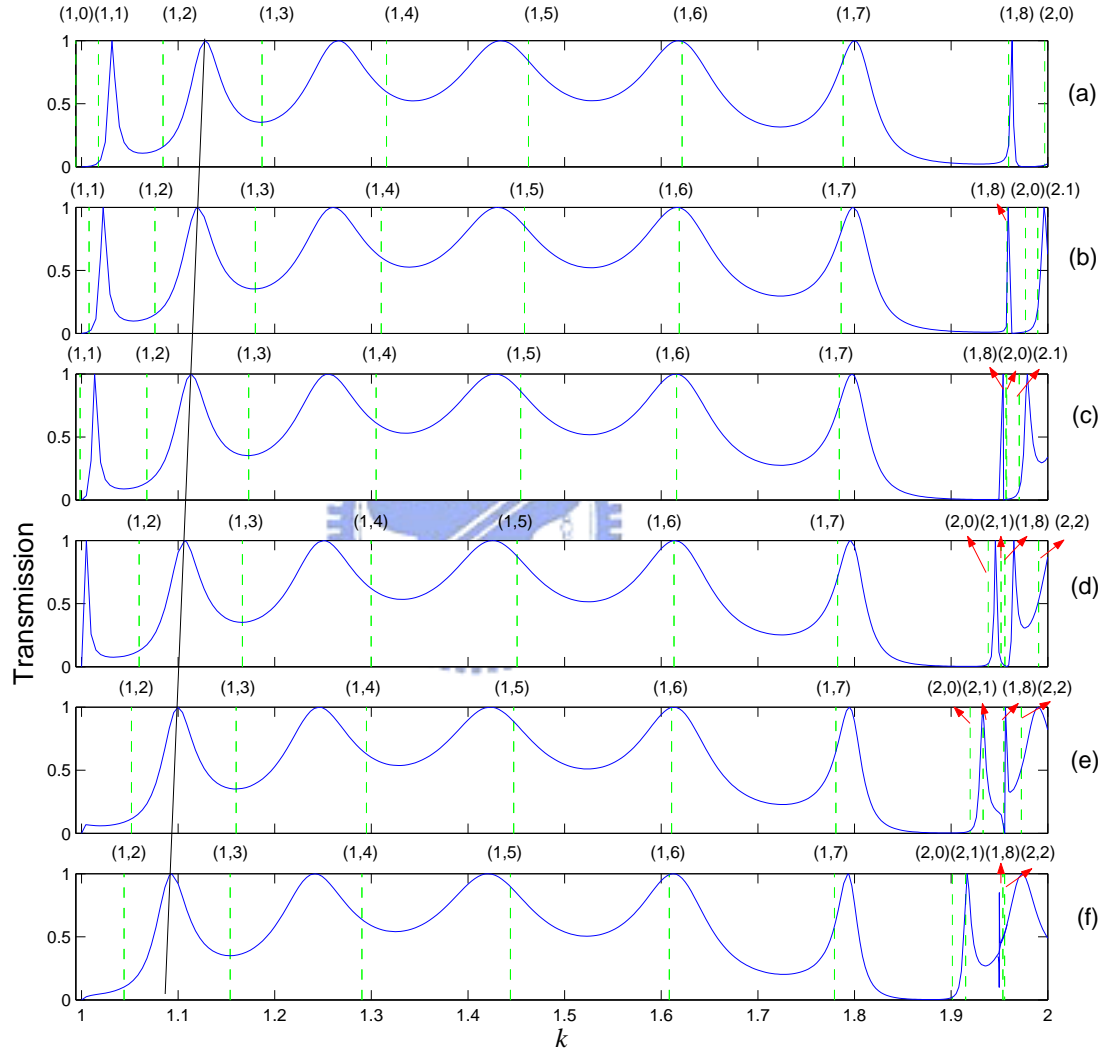
Figure 3.4: The solid line is transmission probabilities as functions of the electron momentum of the OQR of $r_1 = 1$, $s = 1$ and $\theta = \pi$, for different $r_2 = 1$(a), 0.99(b), 0.98(c), 0.97(d), 0.96(e), 0.95(f).
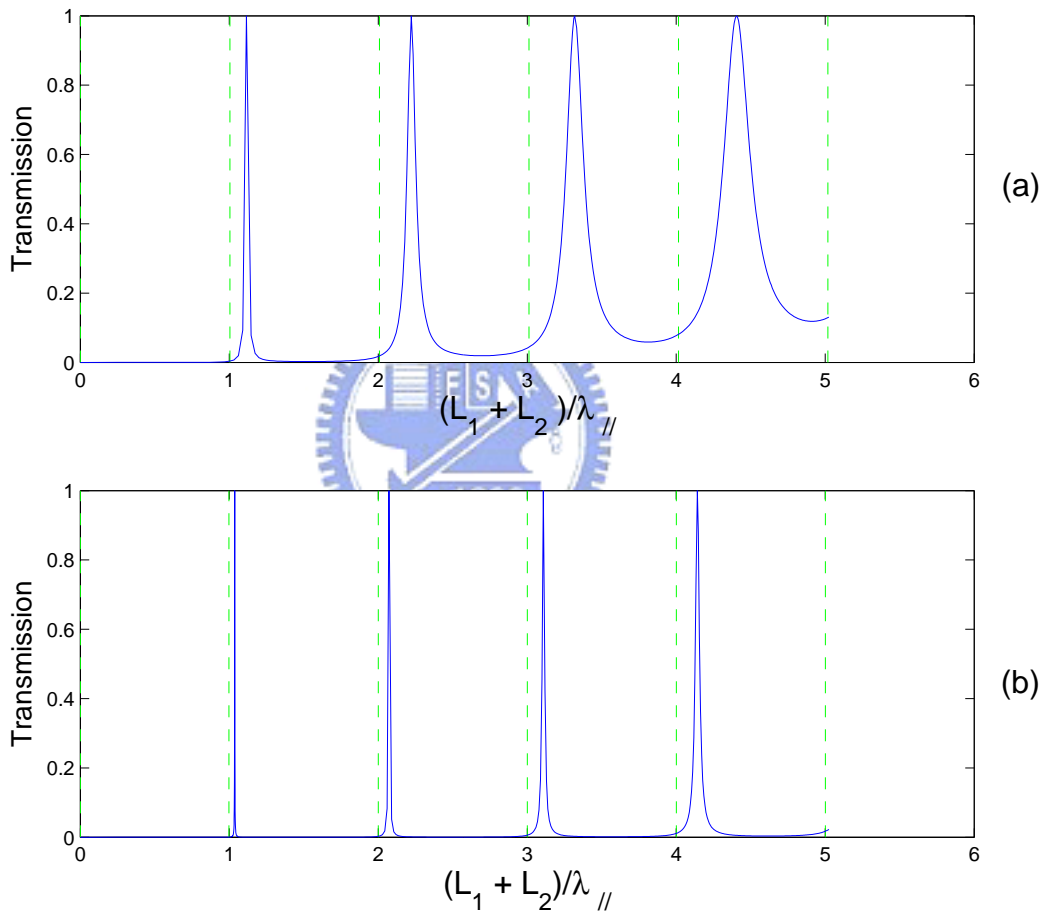
Figure 3.5: The solid line is transmission probabilities as functions of $(L_1 + L_2)/\lambda_{//}$ of the OQR of $\theta = \pi$, for (a)$R/s = 3.5$, (b)R/s $= 9.5$

shift toward the left to be close to confined state of close ring , when the channel narrow
down. And the confined states of close ring are dashed line in Fig. 3.5, and those dashed
line are very close $(L_1 + L_2)/\lambda =$ integer. It seems that the number of waves in the ring
is n when $(L_1 + L_2)/\lambda = n$.

In section 3.2, we found that the Fano structure can be tuned by change geometry
symmetric. Here, we would like to see the change of the Fano structure as approaching to
1D case. Fig. 3.6, shows the transmission probabilities for the case of asymmetrical arms.
From Fig. 3.6, it is seen that the Fano structure become very sharp when the channel is
narrower. But the Fano structures do not shift their position when the channel narrows
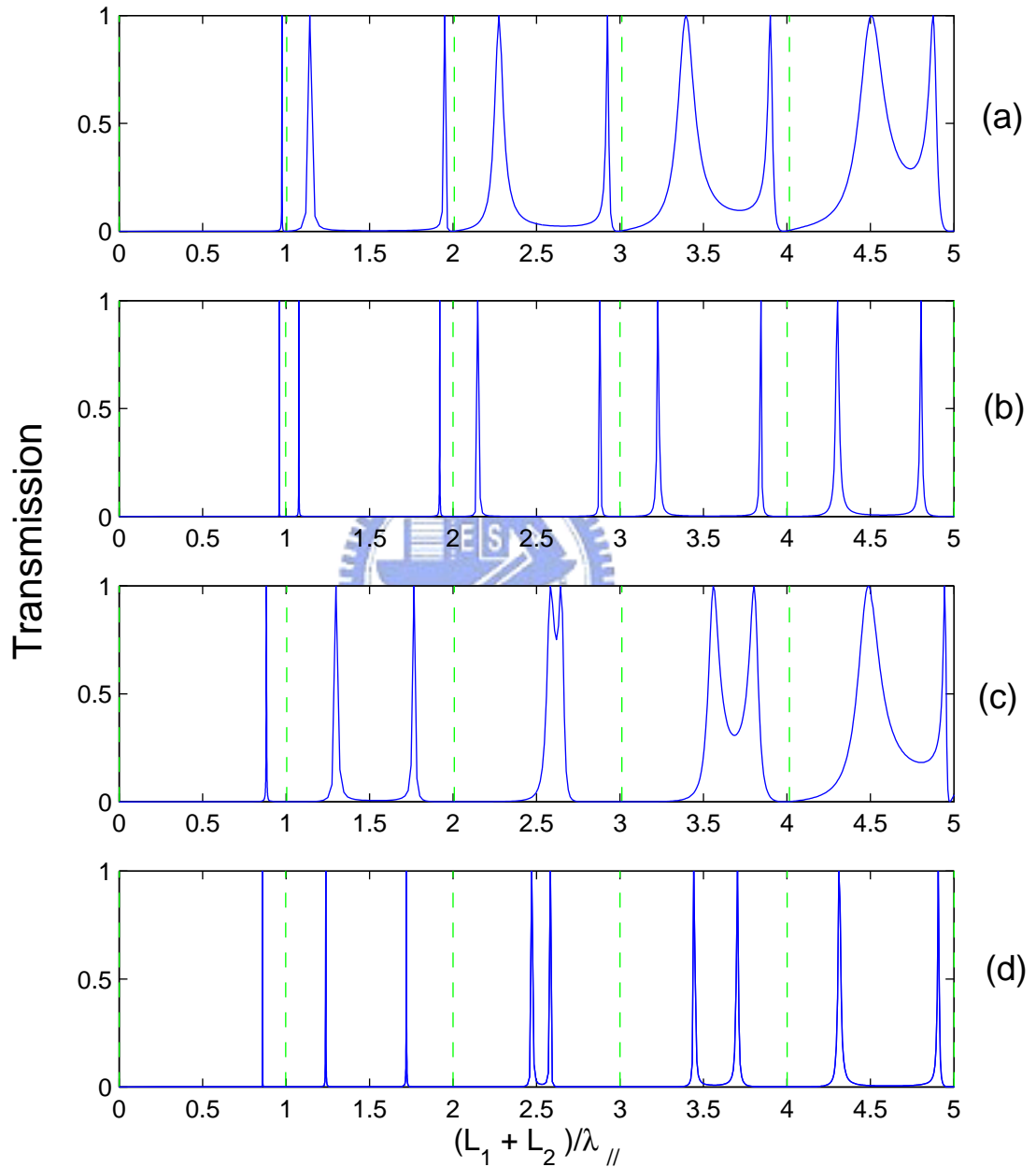down. This is different with the resonance peaks.

Figure 3.6: The solid line is transmission probabilities as functions of $(L_1 + L_2)/\lambda_{//}$ of the OQR for (a)$R/s = 3.5$, $L_1/L_2 = 0.9$ (b)$R/s = 9.5$, $L_1/L_2 = 0.9$, (c)$R/s = 3.5$, $L_1/L_2 = 0.7$, (d)$R/s = 3.5$, $L_1/L_2 = 0.7$

Chapter 4

Numerical results with finite magnetic field
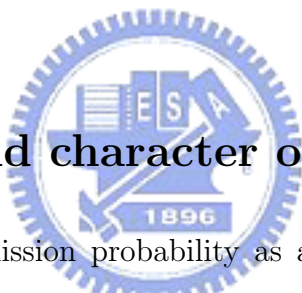
4.1 Magnetic field character on quantum transport

Figure 4.1 shown the transmission probability as a function of Φ/Φ_0 for an AB ring, the system parameters $r_2 = 2$, $r_1 = 1$, $\theta = \pi$ and $k = 1.182$, where Φ is flux through the ring section area and $\Phi_0 = h/2e$ is flux quantum. Form Fig. 4.1 we see that T changes periodically with magnetic field, which is basic characteristic of the AB ring. The oscillating period is $2\Phi_0 = h/e$. This is known as the (h/e) AB effect since one cycle of oscillation corresponds to a change in the enclosed magnetic flux ($\Phi = BS$),where S is the area of the ring. Moreever we can see that the peak of periodic oscillation may split into two peaks at $\Phi/\Phi_0 \geq 16$ see Fig. 4.1, then the periodic oscillation are disappearing at large magnetic field.

4.2 Momentum characteristics on quantum transport

The Fig. 4.2 show that the transmission of an OQR in weak magnetic field ($\Phi_0/\Phi = 0.48$, dashed-dot line) and in zero magnetic field ($\Phi/\Phi_0 = 0$, solid line). Comparing the
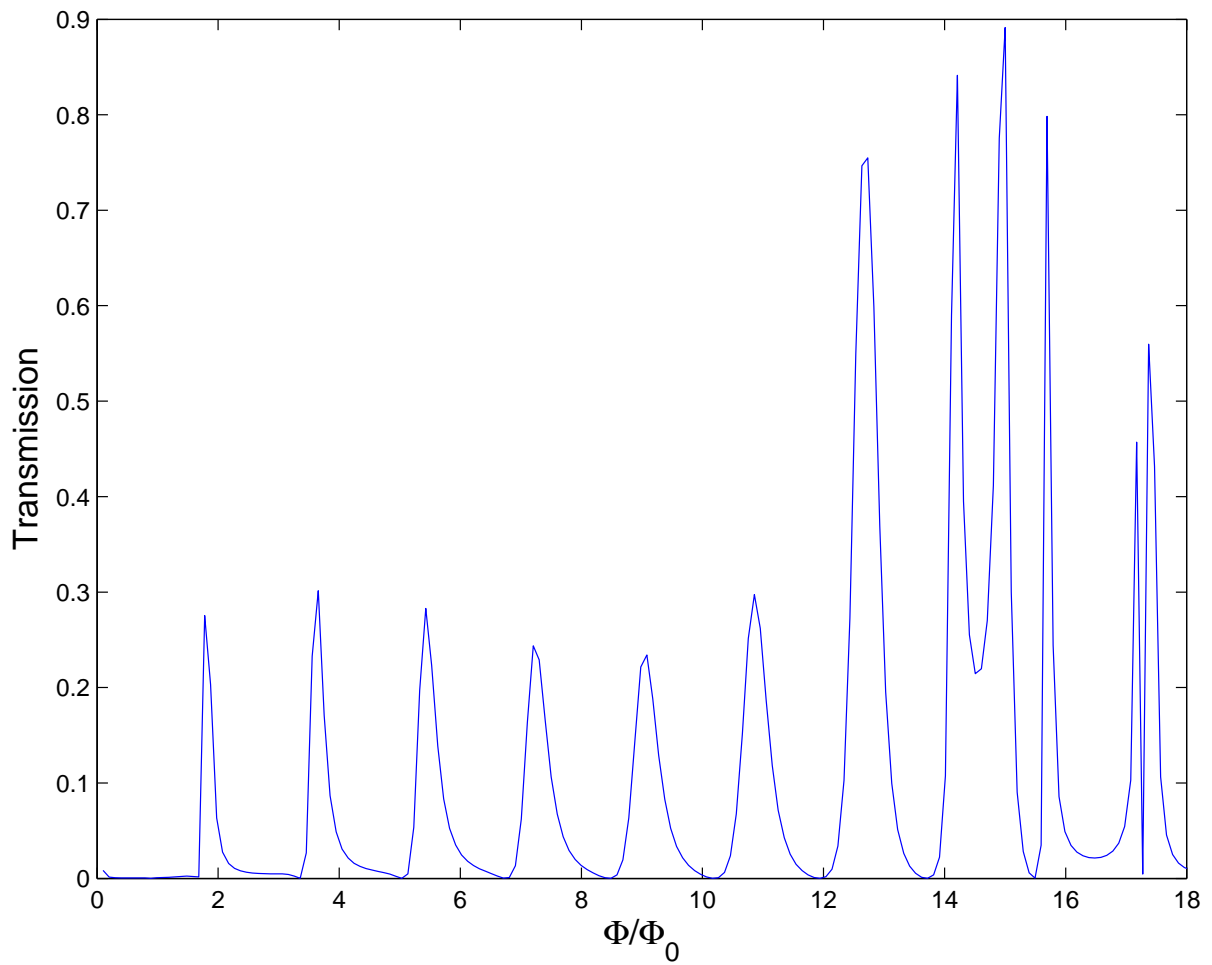
Figure 4.1: The transmission probability as a function of Φ/Φ_0 for an AB ring, the parameters $r_2 = 2$, $r_1 = 1$, $\theta = \pi$ and $k = 1.182$.

transmission of an OQR in weak and zero magnetic field, we can find that there are 14 peaks in weak magnetic filed and 7 peaks in zero field. It is shown that each peak has been splitted into two peaks when weak magnetic field is applied. And it can be also seen that there are Fano structure, locate at the bound states of a corresponding close ring.

For the case of low magnetic field, if we change the angle θ between the two leads of connected from the OQR, the transmission characteristics are shown in Fig. 4.3. From the Fig. 4.3, it is seen that the value of dip with transmission zero are increased by varying θ from π. However other shallow dips are decreased. Interestingly the Fig. 4.4 shows that the variation of transmission of OQR with high magnetic field, when we change θ. Then it show that those transmission in Fig. 4.4 only change a little as varying the angle θ. Hence, it seems that the interference effect are not obvious at large field.
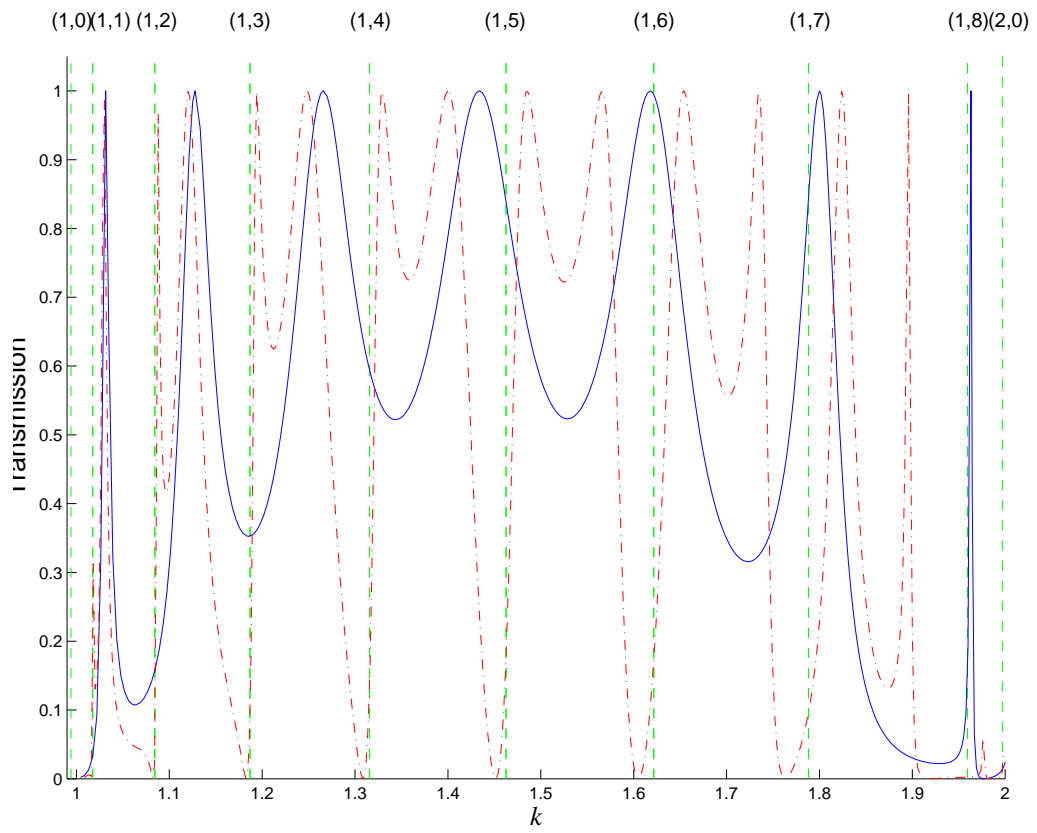
Figure 4.2: The transmission of an OQR in weak magnetic field ($\Phi/\Phi_0 = 0.48$, dash-dotted line) and in zero magnetic field ($\Phi/\Phi_0 = 0$, solid line)
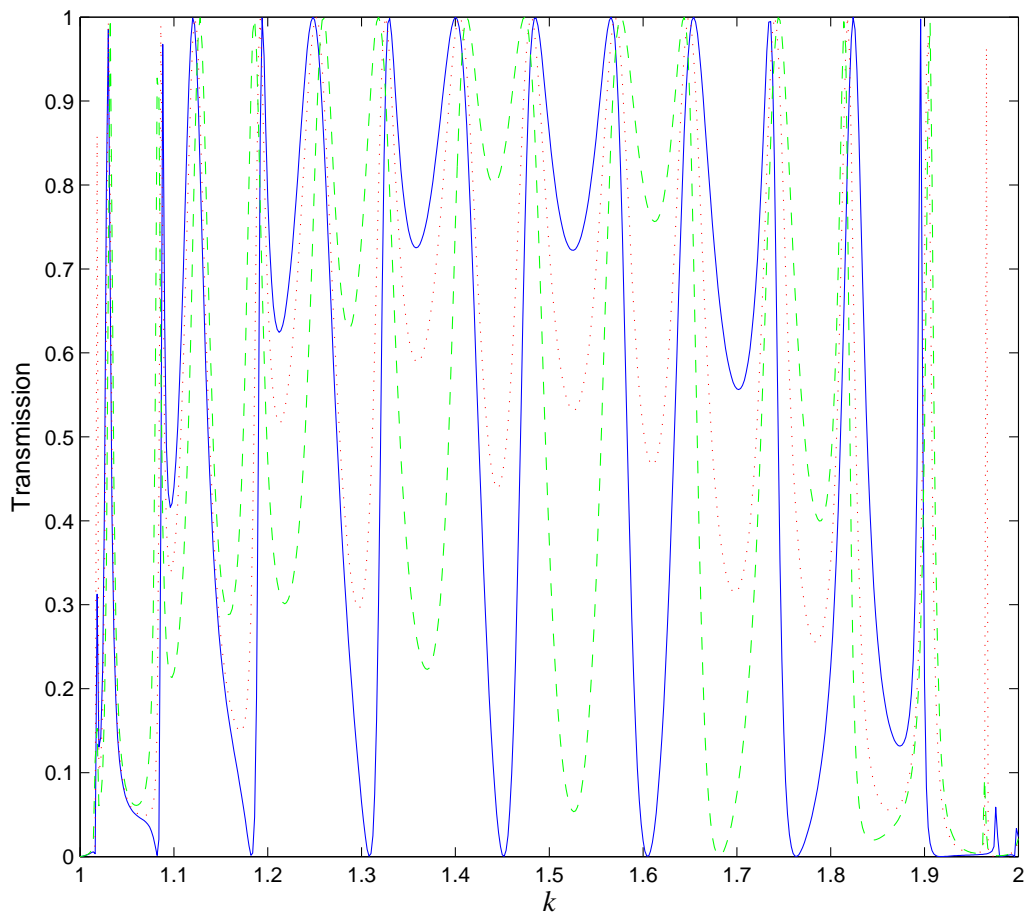
Figure 4.3: The transmission of an OQR $r_2 = 2$ and $r_1 = 1$ in lower magnetic field ($\Phi/\Phi_0 = 0.48$)for different $\theta = \pi$(solid line), 0.96π(dotted line), 0.92π(dashed line).
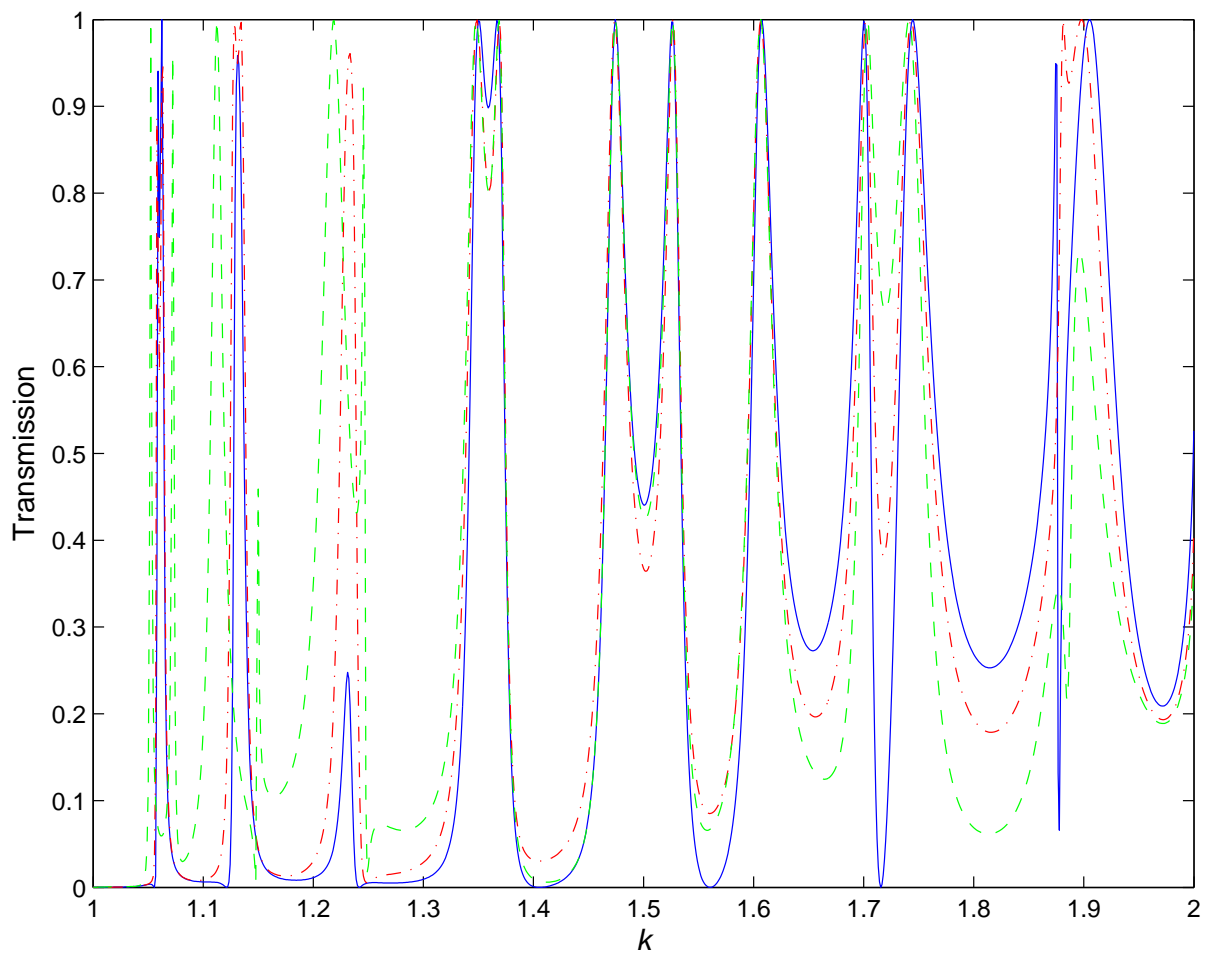
Figure 4.4: The transmission as a function of momentum k. The parameters are $r_2 = 2$, $r_1 = 1$,and $k = 1.182$ in higher magnetic field $(\Phi/\Phi_0 = 9.87)$for different $\theta = \pi$(solid line), 0.97π(dash-dotted line), 0.8π(dashed line).

Chapter 5

Numerical results with magnetic flux

5.1 Comparison with the 1D result

In this chapter, we show the result of an open quantum ring with a magnetic flux in center of ring. First, we compare our schemes with the 1D calculation in a chosen type of system. The way that we calculate the transmission probability for a 1D ring connected to two leads, which is the simplest multiply connected 1D system, using our connection schemes at the three-leg junction (Y junction) [23].

Fig. 5.1 shows the transmission probabilities obtained by different schemes. We have considered different flux $\Phi/\Phi_0 = 0 - 2.0$, and in each case we have presented the result of the 1D scheme with $r = 3.5$ and the results of the Q1D scheme with $r_2 = 4$ and $r_1 = 3$. It is seen that in all cases, the difference between the Q1D and 1D results is slight in the scale of this graph. There are good comparisons between the results due to Q1D scheme and the 1D calculation.

5.2 Magnetic flux character on quantum transport

Fig. 5.2 presents the transmission probabilities of open quantum ring with $r_2 = 2$, $r_1 = 1$ and $k = 1.11$. As expected the transmission show Aharonov-Bohm oscillations. From
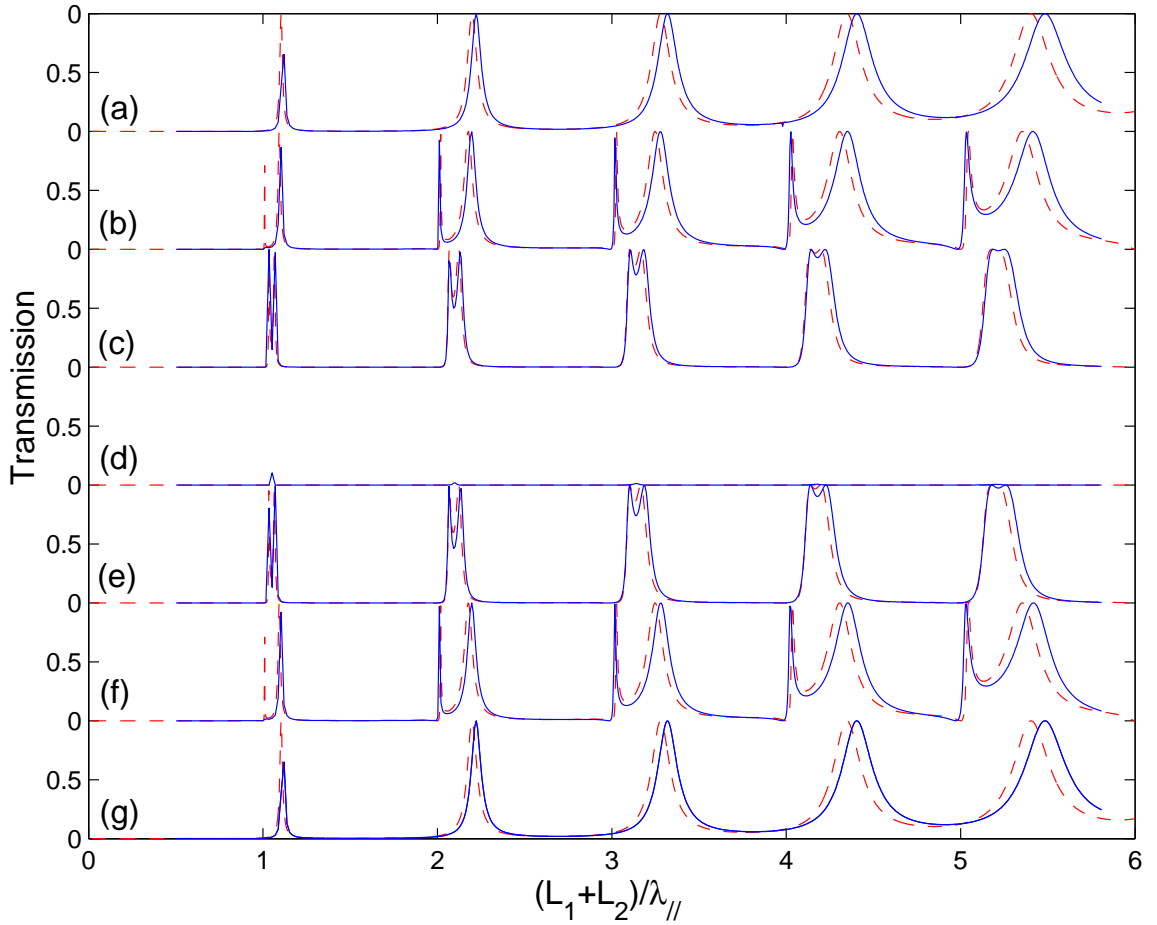
Figure 5.1: The transmission probability T is plotted versus the dimensionless longitudinal wave number in Q1D scheme ($r_2 = 4$, $r_1 = 3$, solid line) and 1D($r = 3.5$, dash line) scheme [24], for different flux $\Phi/\Phi_0 =$(a)2.0, (b)1.6, (c)1.2, (d)1.0, (e)0.8, (f)0.4, (g)0.

Fig. 5.2, the oscillating period is $\Phi/\Phi_0 = 2(\Phi_0 = h/2e)$. Moreover, there are two kinds of strange dips. One is the value of dip equals zero and another is that the minimum value of dip is form of envelope.

Then we choose some dips and peaks, and plot wave function probability at the maximum value of peak and the minimum vale of dip. They are shown in Fig. 5.3. For peaks, the wave function at $\Phi/\Phi_0 = $ (a)12.93 and (c)14.97 are seem that electron like to exit from lower branch and stay on upper branch. On the contrary, the wave function at $\Phi/\Phi_0 = $ (b)13.21 and (d)15.21 seem that like to exit from upper branch and stay on lower branch. For dips, the wave function probability at upper and lower branch for $\Phi/\Phi_0 = $ (e)15.09 and (f)14.1 are symmetry. It differs from the wave function at peaks.
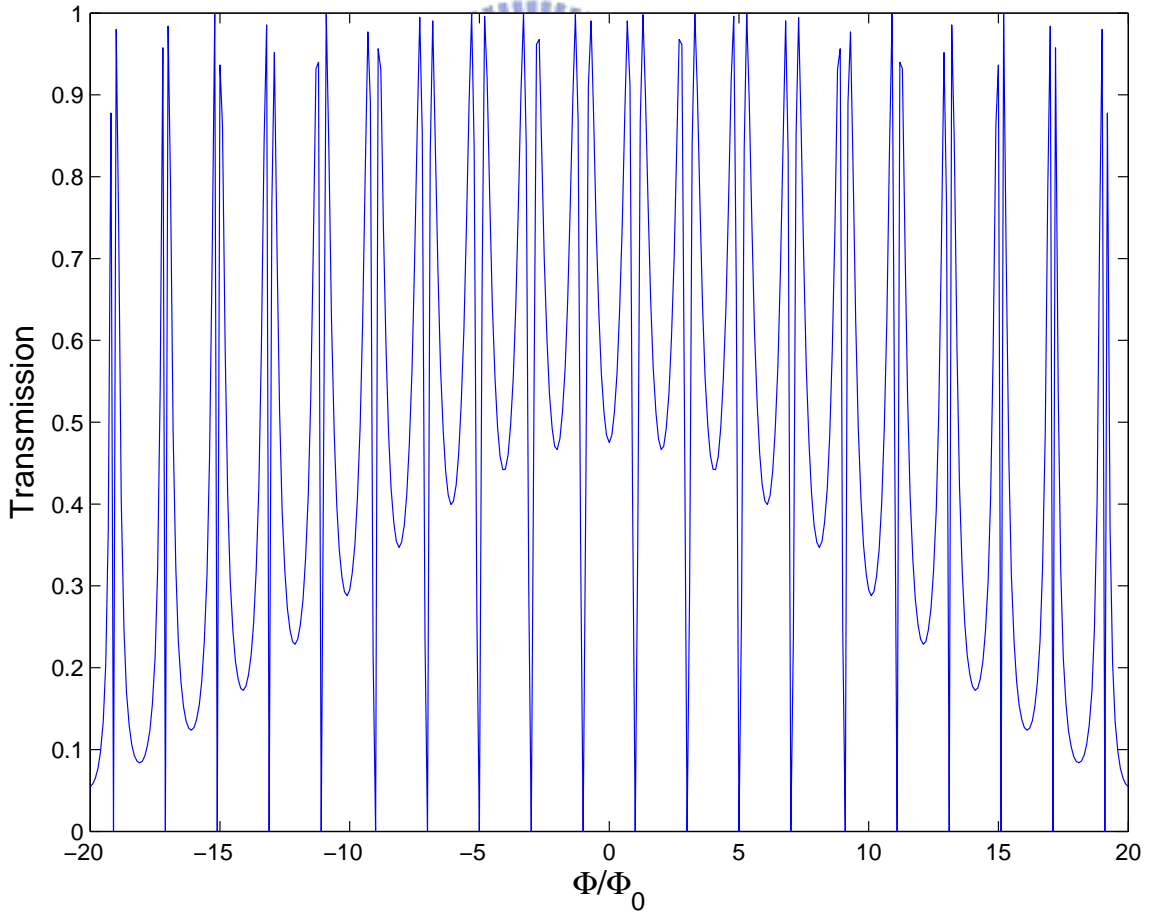

Figure 5.2: The transmission probability as a function of Φ/Φ_0 for an OQR with a magnetic flux in center of ring , the parameters $r_2 = 2$, $r_1 = 1$, $\theta = \pi$ and $k = 1.11$.
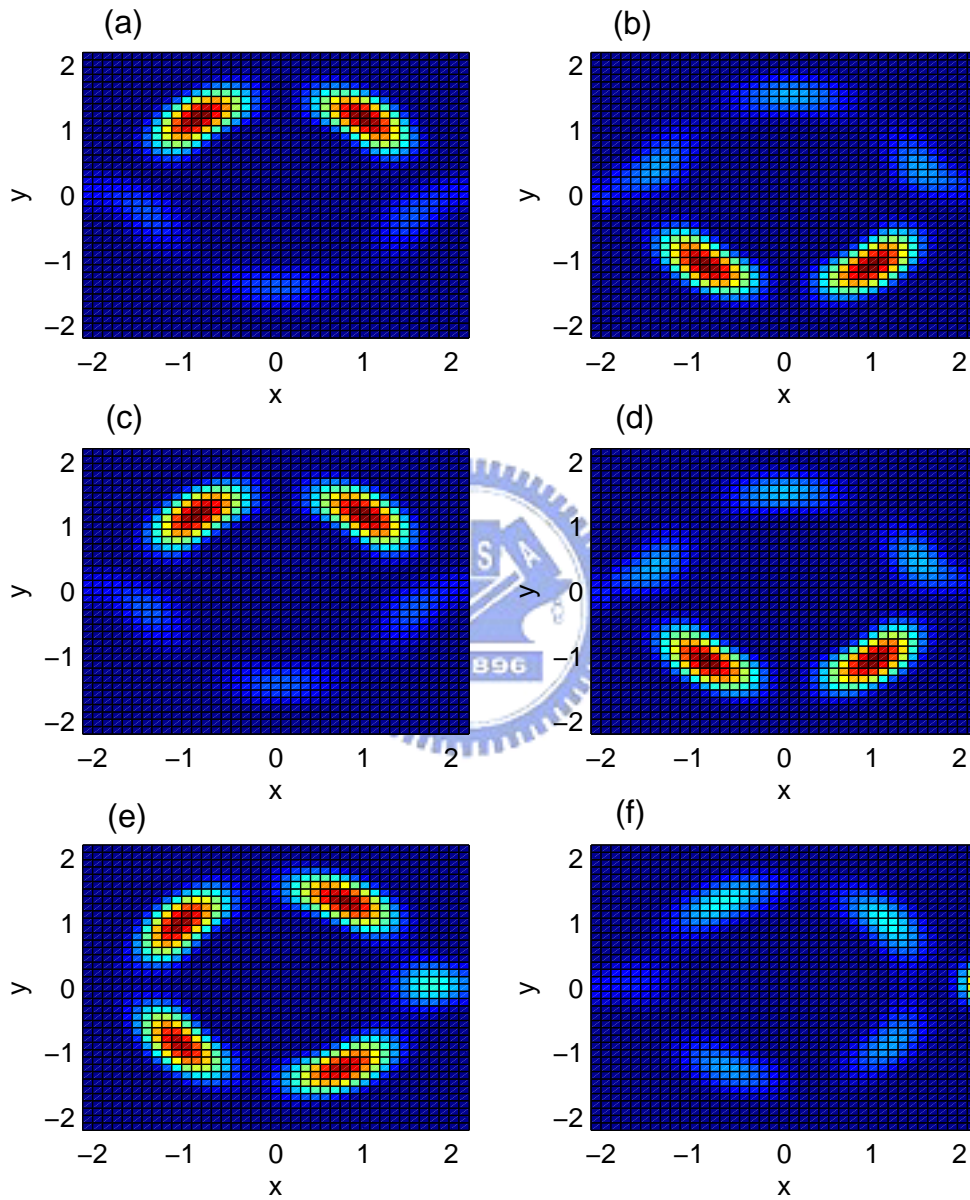
Figure 5.3: The wave function of Φ/Φ_0= (a)12.93, (b)13.21, (c)14.97, (d)15.21, (e)15.09, (f)14.1, for $r_2 = 2$, $r_1 = 1$, $s = 1$, $k = 1.11$ and $\theta = \pi$

Chapter 6

Conclusions and future work

Throughout the thesis, the quantum transport properties through a OQR are calculated and numerically analyzed. We have found that the resonant peaks correspond to the bond states of a close ring. Moreover, we can tune the Fano structure from broad to sharp by varying the symmetry of OQR and turn the Fano structure from sharp to broad by widening the channel width of the ring. Then approaching to 1D case, the resonance peaks become shaper and shift toward the left to be close to bound of close ring, when the channel narrow down. We have found that the AB effect when the external field are applied in the ring and the oscillating period $T_p = 2\Phi_0 = h/e$. It should be noted that the periodic oscillations are disappear at high magnetic field. If we change the angle θ of two lead for low and high magnetic field, we can found that it is sensitive to changing angle θ for small magnetic field but not for large magnetic field. In the thesis, a number of interesting phenomena on quantum transport through an OQR are observed. For the case of zero magnetic field, we have found that the transmission resonances a function of energy has only one missing to match with the bound-state levels of a close ring. The physics behind is still not very clear, and our group member will make diligence on the detail transport mechanisms through the OQR systems. Further studies such as spin-orbit interaction, and time-dependent modulation will be studied in the near future.

Bibliography

[1] A. Lorke, R. J. Luyken, A. O. Govorov, J. P. Kotthaus, J. M. Garcia,and P. M. Petroff, Phys. Rev. Lett. **84**, 2223 (2000).

[2] J. M. Garcia, G. Medeiros-Ribeiro, K. Schmidt, T. Ngo, J. L. Feng,A. Lorke, J. Kotthaus, and P.M. Petroff, Appl. Phys. Lett. **71**, 2014 (1997).

[3] R. J. Warburton et al., Nature **405**, 926 (2000). A. Lorke et al., Phys. Rev. Lett. **84**, 2223 (2001).

[4] M. Buttiker, Y. Imry, and R. Landauer, Phys. Lett. A **96**, 365 (1983); M. Buttiker, Y. Imry, and M. Ya. Azbel, Phys. Rev. A **30**, 1982 (1984); M. Buttiker, in *SQUID' 85-Superconducting Quantum Interference Devices and Their Applications*, Ed. by H. D. Haklbohm and H. Lubbig (Walter de Gruyter, New York, 1985).

[5] R. A. Webb, S. Washburn, C. P. Umbach, and R. B. Leibowitz, Phys. Rev. Lett. **54**, 2696 (1985).

[6] Y. Aharonov and D. Bohm, Phys. Rev. **115**, 485 (1959)

[7] A.G. Aronov and Y.V. Sharvin, Rev.Mod. Phys. **59**, 755 (1987).

[8] Timp G., Chang A. M., Cunningham J. E., Chang T. Y., Mankiewich P., Behringer R. and Howard R. E., Phys. Rev. Lett., **58** (1987) 2814.

[9] Fuhrer A., Lüscher S., Ihn T., Heinzel T., Ensslin K., Wegscheider W. and Bichler M., Nature (London), **413** (2001) 822.

[10] Pedersen S., Hansen A. E., Kristensen A., Sorensen C. B. and Lindelof P. E., Phys. Rev. B, **61** (2000) 5457.

[11] U. Fano, Phys. Rev. **124**, 1866 (1961).

[12] R. K. Adair, C.K. Bockelman, and R. E. Peterson, Phys. Rev. **76**, 308 (1949).

[13] U. Fano and A. R. P. Rau, in Atomic Collisions and Spectra (Academic Press, Orland, 1986).

[14] F. Cerdeira, T. A. Fjeldly, and M. Cardona, Phys. Rev. B **8**, 4734 (1973).

[15] J. Faist, F. Capasso, C. Sirtori, K.W. West, and L. N. Pfeiffer, Nature (London) **390**, 589 (1997).

[16] G. D. Mahan, Many-Particle Physics (Plenum Press, New York, 1990).

[17] V. Madhavan, W. Chen, T. Jamneala, M. F. Crommie, and N. S. Wingreen, Science **280**, 567 (1998).

[18] J. Li, W. D. Schneider, R. Berndt, and B. Delley, Phys. Rev. Lett. **80**, 2893 (1998).

[19] J. G*ö*res *et al.*, Phys. Rev. B **62**, 2188 (2000).

[20] J. Imry, *in Directions in Condensed Matter Physics*, edited by G. Grinstein and G. Mazenko (Wold Scientific, Singapore, 1986), p. 101; C. W. J. Beenakker and H. Van Houten, Solid State Phys. **44**, 1 (1991); S. Datta, *Electronic Transport in Mesoscopic Systems* (Cambridge University Press, Cambridge, England, 1995).

[21] R. A. Webb, S. Washburn, C. P. Umbach, and R. B. Laibowitz, "Observation of h/e aharonov-bohm oscillations in normal-metal rings", *Phys. Rev. Lett.* **54**, 2696?699 (1985).

[22] V. Chandrasekhar, M. J. Rooks, S. Wind, and D. E. Prober, "Observation of aharonov-bohm electron interference eoeects with periods h/e and h/2e in individual micron-size, normal-metal rings", Phys. Rev. Lett. **55**, 1610-613 (1985).

[23] K. K. Voo, S. C. Chen, C. S. Tang, and C. S. Chu, Phys. Rev. B **73**, 035307 (2006).

[24] The 1D data is due to K.-K. Voo (unpublished).